DIPLOMARBEIT

Titel der Diplomarbeit

"Archaeal community profiling using T-RFLP along a latitudinal transect in the Atlantic Ocean"

Verfasserin

Claudia Christine Sulzer

angestrebter akademischer Grad

Magistra der Naturwissenschaften (Mag.rer.nat.)

Wien, 2013

Constellations.

Table of contents

Zusammenfassung

Marine Archaeen sind in der Wassersäule der Ozeane allgegenwärtig. Mittels T-RFLP (Terminaler-Restriktions-Längen-Polymorphismus) von amplifizierten 16S rRNA Genfragmenten wurde deren horizontale und vertikale Verbreitung entlang eines Transekts im Atlantischen Ozean analysiert. Die anschließende Analyse und Klassifizierung der T-RFLP Fragmente in OTUs (Operationale Taxonomische Einheiten), erfolgte *in silico*. Um eine höhere phylogenetische Auflösung zu erhalten, wurden ergänzend Klon-Bibliotheken angelegt. Die höchste Archaeen-Diversität fand sich im Epipelagial (0-100 m Tiefe, 57 OTUs). Sie nahm gegen die tiefer liegenden Zonen ab; am niedrigsten war die Diversität im Bathypelagial (1000-4000 m Tiefe, 20 OTUs). Hinsichtlich längengrad-bedingter Diversitätsunterschiede innerhalb der einzelnen pelagischen Zonen, zeigten sich folgende Tendenzen: Die Diversität in südlichen ozeanischen Provinzen des Epi-pelagials war höher als in den nördlichen Provinzen. Die nördlichen Provinzen der tiefe-ren Zonen waren hingegen reicher an OTUs als die südlichen Provinzen. Einige OTUs zeigten eine eindeutige Tiefenpräferenz. Insgesamt wurden 67 OTUs detektiert, davon stellten 5 OTUs mehr als 54% der relativen OTU Fragment-Abundanz. 62 OTUs waren wenig abundant, charakterisieren aber spezifische Gemeinschaften. Die durch die Klon-Bibliothek zugewiesenen OTUs waren größtenteils den Euryarchaea (Marine Gruppe II Archaea) zuordenbar. Für epipelagische Gewässer zeigte sich, dass Archaeen Ge-meinschaften auf bestimmte ozeanische Provinzen beschränkt sind. Dieser Trend setz-te sich in tiefere, pelagische Zonen fort; die Tendenz nahm jedoch mit zunehmender Tiefe ab.

Abstract

Marine pelagic Archaea are ubiquitously distributed throughout the water column of the world's oceans. The horizontal and vertical distribution of archaeal OTUs (operational taxonomic units) throughout the water column of a latitudinal transect in the Atlantic Ocean was determined via T-RFLP (terminal restriction fragment length polymorphism) of amplified archaeal 16S rRNA gene fragments and supplemented with clone libraries. The highest archaeal diversity was found in epipelagic waters (0-100 m depth; 57 OTUs) and decreased towards deeper layers, being lowest in bathypelagic waters (1,000-4,000 m depth; 20 OTUs). In terms of latitude and depth, archaeal OTU richness lacked a clear trend, but showed a tendency of higher observed and estimated OTU richness in the epipelagic waters of the southern provinces than in the northern provinces. In contrast, higher OTU richness was found in northern provinces in mesopelagic to abyssopelagic waters than in southern provinces. A depth preference of certain OTUs was evident. Five phylotypes made up the majority of relative abundance of OTU fragments, whereas 62 relatively low abundant, rare OTUs accounted for the resulting archaeal diversity. Affiliated sequences to our OTU fragments were mainly assigned to the phylum of Euryarchaea (Marine Group II Archaea). Overall, there is evidence of specific archaeal clusters in distinct oceanic provinces. These clusters of archaeal communities are detected not only in epipelagic but even in meso- and upper bathypelagic waters albeit the number of distinct clusters decreases with depth.

1. Introduction

Until the early 1990's, marine Archaea were thought to be restricted to extreme oceanic environments like anaerobic habitats, hot springs and vents or deep sea sediments which are characterized by halophile, thermophile, sulfur- and methane utilizing archaeal phylotypes. Studies based on the amplification and analysis of phylogenetic markers such as archaeal 16S rRNA gene fragments revealed that planktonic marine Archaea are abundant in marine waters (DeLong 1992, Fuhrman et al. 1992).

It is now well established, that Archaea occur throughout the global ocean in all depth layers (Massana et al. 1998, Karner et al. 2001, Bano et al. 2004, Teira et al. 2006, Wuchter et al. 2006, Varela et al. 2008, Schattenhofer et al. 2009, Amano-Sato et al. 2013, Lekunberri et al. 2013). Representatives of marine Archaea belong mainly to three groups: Euryarchaeota, Crenarchaeota and mesophilic Crenarchaeota Group I, now coined Thaumarchaeota (Brochier-Armanet et al. 2008). Several studies showed that Euryarchaeota are abundant in surface waters, whereas Thaumarchaeota are dominant in meso- and bathypelagic waters (Massana et al. 1997, Massana et al. 2000).

In general, Archaea exhibit a lower richness than Bacteria (Aller & Kemp 2008). While distinct latitudinal differences in bacterial community patterns have been reported for surface and deep waters (Fuhrman et al. 2008, Ghiglione et al. 2012), archaeal community patterns along latitudinal gradients have received less attention. In the present study, we investigate the latitudinal trends in the Atlantic from 64.00°N to 49.55°S covering eight biogeographic provinces as described in Longhurst (Longhurst 2006). Specifically, we aimed at elucidating the distribution of archaeal richness from the euphotic to the abyssopelagic layer from the subpolar Arctic to the subpolar Antarctic waters. Furthermore, we hypothesized that archaeal community composition is more vari-

3

able in the euphotic layer along the latitudinal gradient than in the deeper realms of the Atlantic.

2. Materials and Methods

Sample collection

Water samples were obtained along a latitudinal transect in the Atlantic Ocean from 64.00°N - 49.55°S during three research cruises (Geotraces 1-3) carried out with RV *Pelagia* in April/July 2010 (Geotraces-1, -2) and with RRS *James Cook* (Geotraces-3) in February/March 2011 (Figure 1). Water samples were collected with a CTD (conductivity-temperature-depth; Seabird Bellevue, WA, USA) rosette sampler holding 24 25-L Niskin bottles at 56 stations and 7-8 sampling depths per station from the epipelagic to the abyssopelagic layers. The CTD was also equipped with sensors for chlorophyll fluorescence, turbidity, salinity and O_2. Based on the salinity and temperature characteristics, the major water masses were identified (Tomczak & Godfrey 2003, Van Aken 2010, 2011). Inorganic nutrient concentrations were determined on a TRAACS autoanalyzer on board using spectrophotometric methods (Murphy & Riley 1962, Helder & De Vries 1979, Parsons et al. 1984). Water samples were also collected for microbial abundance and activity; the results of these measurements are reported elsewhere (Bergauer et al., in prep., De Corte et al. 2012). To determine archaeal community composition, 2-10 L of water was filtered through a 0.2 µm pore size polycarbonate filter (47 mm diameter, GTTP Millipore), flash-frozen in liquid N_2 and stored at -80°C until DNA extraction.

DNA extraction and PCR conditions

DNA extraction was performed with an UltraClean Soil DNA isolation kit (Mo Bio Incorporation, CA, USA) following the manufacturer's instructions. The DNA content was spectrophotometrically quantified with the ThermoScientific NanoDrop 2000c by measuring the absorbance at 260 nm wavelength. Samples were kept at -80°C until further analysis.

PCR of the archaeal 16S rRNA gene was performed using the Archaea-specific fluorescently labeled primers 21F-6FAM and 958R-VIC (Table S1) yielding an amplicon of ~ 915 bp length. One PCR reaction (50 µl) consisted of 2 µl of DNA-template, 34.2 µl UV irradiated ultrapure water (Sigma-Aldrich, MO, USA), 0.3 µl of Taq polymerase, 5 µl of the corresponding buffer, 4 µl of dNTP's, 1µl of BSA, 3 µl $MgCl_2$ and 0.25 µl of both primers. PCR was done in duplicate per sample under the following conditions: initial denaturing step at 95°C for 3 min, followed by 30 amplification cycles, denaturing at 95°C for 1 min, annealing at 55°C for 45 sec, elongation at 72°C for 1.5 min and a final elongation step at 72°C for 7 min. PCR amplicons were checked on a 1.2% agarose gel and stained in a freshly prepared 250 ml 1x TBE buffer bath containing SYBR-Gold (10,000x concentrate in DMSO) for 30 min. Duplicate PCR reactions were pooled and purified using the PCR Extract MiniKit (5 Prime) following the manufacturer's instructions with the exception of the final step. The filter-bound DNA was eluted with 2x50 µl UV-irradiated water (Sigma) instead of PEB buffer. The purified PCR amplicons were spectrophotometrically quantified with the NanoDrop.

Terminal restriction fragment length polymorphism (T-RFLP)

For T-RFLP analyses, 200 ng of each purified PCR product was digested with 0.3 µl of the restriction enzyme *Hha*I (Moeseneder et al. 2001) in 0.2 µl of BSA and 2 µl of corresponding buffer at 37˚C for 720 min on an Eppendorf Mastercycler pro S (Table S2). The enzymatic reaction was thermally terminated at 65°C for 20 min and finally cooled down to 4°C. Restriction fragments were desalted with Sephadex (GE Healthcare Life Sciences, Sweden); 4 µl of cleaved PCR fragments were denatured at 95°C for 3 min and stabilized by the presence of 10 µl Hi-Di formamide (Invitrogen) per reaction (Moeseneder et al. 2001). For fragment size detection, 0.40 µl of Gen-eScan1200LIZ (Applied Biosystems) was added as internal standard to each sample. Thereafter, samples were run on a capillary sequencer (Applied Biosystems) following the method of Moeseneder et al. (2001).

Obtained electropherograms were first evaluated with PeakScanner software (Applied Biosystems) and subsequently analyzed with the GelCompar software tool by converting the electropherograms to virtual gel-lanes (Applied Maths, v.6.5). Sample peaks of FAM- and VIC-fragments were normalized to the internal standard (1200 LIZ) and linked to the reference gel. Peaks smaller than 50 bp and larger than 1200 bp were considered as remains of the primer or undigested fragments and hence, were excluded from further analyses. To decrease background noise and smoothen peaks for better peak height resolution, the Wiener cutoff scale and background scale were calculated by the program and subtracted from the peak height. The resulting peaks of FAM- and VIC-labeled 16S rRNA fragments were binned.

Based on the fragment length, binning thresholds were as follows: fragments < 700 bp with ± 1bp difference were assigned to individual operational taxonomic units (OTUs). Within the fragment size range of 700-1000 bp, fragments with ± 3 bp difference were classified as one OTU while fragments ≥ 1000 bp with ± 5bp difference were classified as one OTU (Hewson et al. 2006) The OTUs obtained from FAM- and VIC-

labeled fragments were exported as presence-absence matrix (p/a matrix) and as absolute peak height matrix serving as raw data for further analyses in Excel, Primer6, EstimateS, Statgraphics and SPSS.

Cloning and sequencing of archaeal 16S rRNA genes

16S rRNA clone libraries were established from six samples collected at six stations over a depth range of 50-2800 m. PCR reactions were performed in triplicate, amplifying the archaeal 16S rRNA gene and applying the same conditions as described above. PCR products were checked on a 1.2% agarose gel; triplicate reactions were pooled and purified as described above. Cloning reactions were performed with the TOPO TA Cloning Kit (Invitrogen, Carlsbad, CA, USA) using TOP10 *Escherichia coli* cells according to the manufacturer's instructions. Transformed cells were plated on freshly prepared LB-plates (lysogeny broth) containing 100 mg l^{-1} ampicillin and 40 μl of X-Gal (40 mg ml^{-1}) and incubated overnight at 37°C. After blue-white screening, 50 clones per sample were randomly picked with sterile toothpicks, transferred onto a LB plate (master-plate) and re-grown overnight at 37°C. For screening the correct insert size, M13 PCR was done under the following conditions: one initial denaturing step at 95°C for 4 min, followed by 30 amplification cycles, a denaturing step at 95°C for 1 min, annealing at 60°C for 45 sec, elongation at 72°C for 1.5 min and a final elongation step at 72°C for 7 min using vector binding M13F and M13R primers (Table S1). Amplicons were visualized on a 1.2% agarose gel (SYBR-Gold staining). 285 clones containing the correct insert size were transferred onto sequencer plates and sent for sequencing (GATC Biotech, Germany). Obtained forward and reverse sequences were assembled with CodonCode Aligner (CodonCode Corporation, MA, USA) software (Sintes et al. 2013). Resulting 16S rRNA gene sequences were subjected to reduced redundancy testing of sequences being 90 % similar to each other. Potential chimeric 16S rRNA sequences were excluded with the online tool Check Chimera of the RDP (Cole et al.

2003). For phylogenetic inference, assembled sequences were blasted using the BLAST search engine against public databases in NCBI.

Forty-six clones were again subjected to T-RFLP analysis as described above, except that capillary sequencing was performed with 1µl of digested 16S rDNA product. The peaks assigned to specific archaeal taxa were used to tentatively identify these taxa in the electropherograms of the individual samples collected along the latitudinal transect.

Statistical analysis

In total, 357 samples of 56 stations were analyzed using GelCompar to obtain presence/absence (p/a) matrices after peak assignment of T-RFLP fragments. Samples were assigned to eight biogeographical provinces following the Longhurst classification scheme (Longhurst 2006). Statistical analysis was initially done on four classified depth layers comprising the epi-, meso- bathy- and abyssopelagic realm. Subsequently, eight depth layers were used to resolve depth-related patterns of archaeal communities (Figure 4-6). To test for differences in the number of OTUs obtained between the two primers, a Wilcoxon signed rank test in SPSS (IBM Corporation, NY, USA) was used. Jaccard index-based similarity trees were generated in Primer6 (Primer-E Limited, UK) for identifying the extent of latitude and depth as structuring components in archaeal communities. Estimations for species richness and species observed (S_{obs}) were performed with EstimateS 7.5.2 (Gotelli 2001) using the bias corrected Chao 2 index and the computed S_{obs}. Changes in archaeal community composition within and between specific depth layers were evaluated using Jaccard similarity via Shared Species observed in EstimateS.

3. Results

Physical and chemical parameters along the latitudinal transect

The mean temperature throughout the latitudinal transect showed specific characteristics in the surface waters of the different biogeographic provinces and rather uniform temperatures in the deep waters with the coldest deep waters at the southern end of the transect representing Antarctic Bottom Water (AABW) (Appendix Table, Figure S1A). Salinity was highest in epipelagic waters, particularly in the gyre provinces such as NASW (36.56±0.06), NATR (36.56±0.30) and SATL (36.65±0.62) (Appendix Table, Figure S1B). Low salinity was associated with Antarctic Intermediate Water (AAIW) centered at around 900 m depth.

Nitrate concentrations were generally low in epipelagic waters particularly in the gyre regions north and south of the equator and increased towards 750-850 m depth (26.93±6.74 µmol kg^{-1}). Below this depth layer, nitrate concentrations decreased slightly and increased again below >5000 m depth reaching highest nitrate concentrations there (32.29 ±1.20 µmol kg^{-1}) (Appendix Table, Figure S1C). Generally, the South Atlantic exhibited higher nitrate concentrations, which extended in deeper layers towards the north representing the flow of Antarctic Intermediate Water (AAIW) and AABW (Appendix Table, Figure S1C).

Phosphate concentrations showed a similar latitudinal and vertical distribution pattern as nitrate with highest mean concentrations at depth >5000 m (2.23±0.10 µmol kg^{-1}) (Appendix Table, Figure S1D). Silicate concentrations were generally high in the SANT province, particularly in the layers > 5000 m (119.85±9.19 µmol kg^{-1}) decreasing steadily towards the equatorial region (Appendix Table, Figure S1E) reflecting the high silicate concentration of the Antarctic water masses (AAIW, AABW) flowing to the north.

The apparent oxygen utilization (AOU) in the Atlantic intermediate and deep waters was characterized by a higher AOU under the gyres north and south of the equator

(≈ 175 µmol kg^{-1} at 375-600 m depth) and generally increased towards the south as North Atlantic Deep Water (NADW) ages (Figure S1F). The waters below 1000 m depth south of 35°S exhibited AOU values of about 150 µmol kg^{-1} (Figure S1F).

Latitudinal and vertical distribution of archaeal OTUs

In total, 73 OTUs were obtained with 21F-FAM (range 72-945 bp) and 55 OTUs with 958R-VIC (range 80-914 bp) (data not shown). Six OTUs were excluded from the analyses as they were singletons, hence appearing only once within the presence/absence (p/a) matrix of all samples. The relative rank abundance of all OTUs of the 357 samples showed, that the five most frequently present OTUs constituted 54% of relative OTU abundance (Figure S4), while each of the remaining 62 OTUs constituted <2 % (Figure S4) of relative OTU abundance.

On a latitudinal scale, the number of OTUs obtained for epipelagic waters was significantly higher with the primer 21F-FAM than with 958R-VIC (Wilcoxon signed rank, P < 0.01), whereas the number of OTUs for mesopelagic and bathypelagic waters was higher with the primer 958R-VIC than with 21F-FAM (for both water layers: Wilcoxon signed rank, P < 0.001). The same trend as for the meso- and bathypelagic waters was found for the abyssopelagic realm (Wilcoxon signed rank, P= 0.02) (Figure 2).

In epipelagic waters, the number of OTUs obtained with the primer 21F-FAM was significantly higher in the provinces around the equator (NATR, WTRA, SATL and SSTC) than with the primer 958R-VIC while no differences in the number of OTUs obtained with the two primers were detected in the subpolar provinces (Table S3). In mesopelagic waters, the number of OTUs obtained with the primer 958R-VIC was always higher than with 21F-FAM except for the NASW (Table S3). Also in bathypelagic waters, the number of OTUs obtained with the primer 958R-VIC was higher than with the primer 21F-FAM while in the abyssopelagic layer, the number of OTUs derived with the two primers was not significantly different except for the SSTC (Table S3).

Estimated archaeal richness versus Sobs

Throughout all depth layers, archaeal richness was highest in epipelagic waters (Figure 3A-D). In these epipelagic waters, NATR exhibited the highest OTU richness (Chao 2 mean OTUs±SD: 70±21); the polar provinces ARCT and SANT differed notably in their OTU richness (ARCT: 7±1; SANT: 23±4). In mesopelagic waters, highest richness was found in NASW (29±5 OTUs) while bathypelagic waters did not show clear trends in archaeal richness throughout the transect (Figure 3C). In abyssopelagic waters, a higher OTU richness was detected in the northern provinces (Figure 3D).

Obtained species observed (S_{obs}) (Figure S2) for each pelagic layer revealed the highest S_{obs} number of OTUs in epipelagic waters (OTUs S_{obs}: 57) and lowest in bathypelagic realms (20 OTUs) with meso- and abyssopelagic OTUs close to that of the bathypelagic realm (Figure S2).

Changes in archaeal community composition along the transect

Similarity trees based on Jaccard analysis for the epi- to the abyssopelagic communities are shown in Figure S3A-D. In epipelagic layers, archaeal communities exhibited generally a lower similarity than in the other water layers, however, one cluster of archaeal communities of low latitude provinces (NATR, WTRA, SATL and SSTC) and one of high latitude regions (ARCT, NADR and SANT) were clearly identifiable (Figure S3A). The four most abundant OTUs within all the samples of the euphotic zone occurred in both clusters (31, 38, 39, and 40; data not shown). Low latitude provinces were generally richer in archaeal diversity than higher latitude provinces as OTUs 1-23 and 57-69 occurred only here. Within the ARCT-NADR-SANT cluster, SANT showed relatively more rare OTUs than ARCT and NADR as eight OTUs were present only in SANT (16, 17, 22, 27, 43, 44, 48 and 53). The distinct archaeal cluster of the euphotic NASW was due to the absence of OTUs, which were always present in the ARCT-NADR-SANT and the NATR-WTRA-SATL-SSTC cluster and a relatively higher richness

of OTUs with a fragment length of >660 bp. The low latitude cluster was dominated by samples originating from WTRA and SATL (Figure S3A). Despite for one SANT sample, OTU 48 was restricted to WTRA and SATL whereas OTUs 24-29 and 60-69 were only found in NATR and SSTC.

Mesopelagic waters exhibited two archaeal community clusters: one in NATR and one cluster dominated by NASW (Figure S3B) samples. Five OTUs were ubiquitously distributed throughout all provinces within this layer (31, 38, 39, 59 and 60). The archaeal community of the mesopelagic NASW was rather dissimilar to the archaeal communities from other provinces (Figure S3B). OTUs 52-57 and 66-69 were almost restricted to NASW; OTU 62 appeared only in NASW. OTUs 41-43 were uniqueNASW and NATR, OTUs 46 and 47 almost restricted to NATR.

In the bathypelagic waters, two (sub)tropical archaeal clusters were discernable, one dominated by SATL and one by NATR; another one was dominated by NASW and one by SSTC, ARCT and NADR (Figure S3C). Five archaeal OTUs were ubiquitously present in all provinces (33, 38, 39, 44 and 60). Though separated into two (sub)tropical clusters, both clusters exclusively shared the a large number of OTUs. All samples of these clusters originated from different water masses and depths. Compared to the tropics, a lower diversity was found in the ARCT-NADR and SSTC-SANT cluster in bathypelagic waters. The bathypelagic SSTC-SANT cluster generally showed a lower diversity than the ARCT-NADR cluster. OTU 44 occurred in all the provinces but was rare in the bathypelagic SSTC-SANT cluster. OTU 56 was present only in the bathpelagic waters of the NASW and NATR province.

The archaeal community of the abyssopelagic waters was characterized by three distinct archaeal clusters: the NASW-NATR, WTRA-SATL and NADR-SSTC-SANT cluster (Figure S3D). Five OTUs were ubiquitously present (31, 38, 39, 44 and 60). Three OTUs were almost exclusively present in the NASW and NATR province (32, 59 and 68). OTU 43 only appeared in NATR, WTRA and SATL.

The variability of the archaeal community within the individual depth layers is shown for each oceanographic province separately (Figure 4). Generally, the archaeal communities of the 50 m layer tended to be less similar, those of the deeper layers more similar. The lowest similarity within the 50 m layer was found in NATR (Jaccard similarity, 28%), the highest in NASW (71%). Comparing the tropical provinces NATR and WTRA, the archaeal communities of NATR exhibited a lower similarity throughout all depths than those of WTRA (Figure 4). Compared to the ARCT, the archaeal communities of the SANT exhibited a lower similarity until 250 m depth (Figure 4).

Changes in the archaeal community composition from one depth layer to the one underneath were detected in 50 m to 250 m layers, particularly pronounced in NATR (community similarity 50 m to 250 m: 14%) and SATL (15%) (Figure 5). In the tropical provinces, the archaeal community composition among the different depth layers were less similar in the NATR than in WTRA province. In polar provinces, the archaeal communities in the different depth layers of the ARCT were more similar until 375 m depth than in the corresponding depth layers of the SANT.

Changes in the archaeal community composition throughout the water column in relation to the community composition of the 50 m layer are shown in Figure 6. Overall, the lowest similarity in archaeal communities of all depth layers to that from 50 m depth was detected in NATR (community similarity range of all layers to 50 m: 8-14%) and SATL (9-15%), whereas the highest community similarity to the 50 m depth layer was found in ARCT (33-62%). In the tropical provinces, archaeal communities in the NATR exhibited a lower similarity than those of the WTRA. The depth stratification of the archaeal communities differed between the ARCT and SANT; the archaeal community of the 375 m layer was more similar to that of the 50 m layer in the ARCT than in the SANT.

Distribution of OTUs phylogenetically assigned by clone libraries and sequencing in the different water layers, provinces and water masses

From six samples, 285 clones were randomly picked and sequenced. Forty-six clones were subjected to subsequent T-RFLP analyses. Thirteen T-RFLP peaks were tentatively identified, representing mainly the more ubiquitously present Archaea, particularly the Euryarchaeota (Figure S4). Three of the identified peaks were affiliated to uncultured marine Archaea and one to Crenarchaeota.

Three of the thirteen affiliated OTUs (31, 38 and 39) occurred ubiquitously (data not shown) (Figure S4). OTU 43, affiliated to Crenarchaeota was absent in epipelagic waters and appeared within NATR in the mesopelagic layer and in the (sub)tropical provinces in the bathy- and abyssopelagic layer. The water masses constituting these layers are NADW and AABW. OTU 32 was predominantly found in the meso- and abyssopelagic layer of the NADR, NASW and NATR province. These layers are fed mainly by the water masses NACW and NADW. Euryarchaeal OTUs 36 and 37 were prominent in the epipelagic waters of all provinces as well as in the mesopelagic waters of the northern provinces, which are supplied by water masses of the Irminger Current, LSW (Labrador Sea Water), NAC (North Atlantic Current) and NACW. Also, euryarchaeal affiliated OTUs 1, 6, 10 and 54 were restricted to epipelagic waters. OTU 1,6 and 10 occurred only in (sub)tropical provinces, whereas OTU 54 occurred in all provinces except in the ARCT. OTU 69 was exclusively present in epi- and mesopelagic waters of the NASW and NATR province.

4. Discussion

In general, prokaryotic richness is higher in Bacteria than in Archaea in the open ocean (Aller & Kemp 2008). This was also found along the transect covered in the Atlantic by Geotraces 1-3 (Bergauer et al., in prep.).

A higher number of 16S rRNA gene fragments were detected with the forward primer than with the reverse primers in epipelagic waters, whereas deeper waters were significantly higher in OTUs obtained with the reverse primer (Figure 2). Similar findings were reported by Moeseneder et al. 2001.

Changes in archaeal richness with depth and latitude

In the present study, archaeal richness decreased with depth (Figure S2), which agrees with previous studies from the Mediterranean Sea and the open Atlantic (De Corte et al. 2009, Lekunberri et al. 2013).

Figure 3A-D shows the estimated archaeal richness for several pelagic layers and provinces. Overall, one has to keep in mind that the cruises were carried out at different seasons; the northern hemisphere was sampled between April and July thus, at the peak of the productive season. Samples in the southern hemisphere were collected in February/March corresponding to late fall and therefore, at the end of the productive season. Hence, potential seasonal community shifts particularly in the epipelagic layer might have occurred. In epipelagic waters, a higher archaeal richness was obtained in the southern Atlantic; NATR exhibited the highest estimated richness (70±21 OTUs) and in the SANT, archaeal richness (23±4 OTUs) was considerably higher than in the ARCT (7±1 OTUs) (Figure 3A). Overall, there was a general trend discernable with an increasing archaeal richness from high to low latitudes in the epipelagic waters, a trend which has been found also in Bacteria (Fuhrman et al. 2008, Ghiglione et al. 2012) as well as in eukaryotes including metazoans (Roy et al. 1998, Hillebrand 2004).

While the ARCT province was sampled in late spring to summer, the SANT province was sampled in austral fall. Mean chlorophyll *a* concentration is similar in the ARCT (0.30±0.10 µg dm^{-1}) and the SANT (0.28±0.18 µg dm^{-1}). Whether sampling these two polar provinces in different seasons is the reason for the higher archaeal richness in the SANT than in the ARCT (Figure 3A) remains speculative.

Meso- and abyssopelagic waters exhibited a higher estimated archaeal richness in the northern than in the southern hemisphere, whereas bathypelagic waters did not show any latitudinal trends (Figure 3B-D). Interestingly, while archaeal richness increased from polar regions to the equatorial regions, crenarchaeal abundance was found to decrease from 65°N to 5°N in the Eastern North Atlantic in the meso- and bathypelagic waters and was positively correlated to ammonia concentrations, which decrease towards lower latitudes (Varela et al. 2008). As ammonia concentrations are higher in mesopelagic waters of the southern Atlantic coinciding with lower archaeal richness, it appears that high ammonia concentrations are linked to low archaeal richness.

Community composition and similarity trees of the four pelagic layers

In order to determine the extent of variations in archaeal community composition along a latitudinal gradient, similarity trees were established (Figure S3A-D). These similarity trees established for each pelagic layer revealed a clustering according to biogeographic provinces (Figure S3A-D). Within the epipelagic layer, one cluster of ARCT-NADR-SANT archaeal communities and one NATR-WTRA-SATL-SSTC cluster are identifiable (Figure S3A). Bano et al. (2004) compared archaeal communities of the Arctic and Antarctic seas using DGGE. They found most archaeal community members are common to both polar regions in layers deeper than 130 m. However, significant differences in archaeal assemblages were reported for the top 50 m layer. For the ARCT, they did not detect a seasonal pattern for community assemblages, but related the

community composition to depth (Bano et al. 2004). Increasing richness patterns as found for marine Bacteria towards lower latitudes (Fuhrman et al. 2008) are in agreement with our results for Archaea.

Within the mesopelagic realm, NATR and NASW each showed specific archaeal clusters (Figure S3B). The main water mass contributing to the mesopelagic layer of NATR is NACW. Unfortunately, water mass contributions for the mesopelagic layer of the NASW was not as clear as for NATR. However, water masses determined to a large extent the bacterial and archaeal community composition of meso- and bathypelagic waters as shown for the tropical Atlantic (Lekunberri et al. 2013).

The separation of the two (sub)tropical cluster in the bathypelagic water could not be ascribed to water mass or depth; all samples of both clusters originate from different water masses and depth layers. The clustering of widely separated archaeal communities from temperate and subpolar regions indicate that their specific physico-chemical conditions lead to the formation of phylogenetically similar communities even in the deep waters (Ghiglione et al. 2012).

Variability of community composition within and between water layers

Within the different oceanic provinces and within the individual depth layers, the similarity in the archaeal community composition was high in layers below 250 m depth but generally low in surface waters (50 m depth) (Figure 4). It has been shown that bacterial communities are stratified with depth in the oceanic water column (DeLong et al. 2006, Agogue et al. 2011). We obtained a similar depth stratification in archaeal communities (Figure 5). As shown in Figure 5, the similarity of the archaeal communities increases generally with depth indicating that the changes in the archaeal community composition become more subtle towards the deeper layers in the Atlantic. There is, however, a remarkable change in similarity at the 3500 m depth layer in almost all oceanic provinces. In this 3500 m layer, the similarity in the archaeal community is lower

compared to the layer above, indicating an isolation of the AABW to the overlying NADW and limited exchange of Archaea between these water masses (Figure 5). Pronounced changes in the archaeal community composition from the surface waters towards the deep waters are evident for the ARCT, NASW, NATR and SSTC provinces, while the other provinces generally exhibited low archaeal community similarity when related to the community composition of the top 50 m layer (Fig. 6). This pattern again points to a stratification of the archaeal community in the water column of the Atlantic.

Clone library and peak assignment

Six samples with a depth range of 50-2800 m were taken for establishing a clone library. Subsequent peak assignment revealed Euryarchaeota among the dominant phylotypes in the clone libraries. The most abundant archaeal OTU (OTU 31, Figure S4) could not be assigned to a specific archaeal taxon. Remarkably, the majority of the Archaea obtained in the clone library was affiliated to the Euryarchaeota although commonly Euryarchaeota are lower in abundance than Crenarchaeota Marine Group I or Thaumarchaeota in the open oceanic water column (Karner et al. 2001, Varela et al. 2008). Though we could only assign one sequence to Crenarchaeota, their increasing presence in samples towards deeper layers corresponds to previous studies (Massana et al. 2000, Karner et al. 2001, Church et al. 2003).

5. Conclusion

Archaeal richness increased from high to low latitudes most pronouncedly in the euphotic layer with a decreasing latitudinal richness trend towards the abyssopelagic layers. Along the longitudinal transect through to Atlantic, we could clearly identify clustering of archaeal communities throughout the water column following the Longhurst oceanographic provinces. Hence, it appears that archaeal community composition in the bathy- and abyssopelagic waters is clustered in a similar way as euphotic and mesopelagic waters despite the more stable physico-chemical conditions in the deep waters leading to a pronounced depth stratification of the archaeal community.
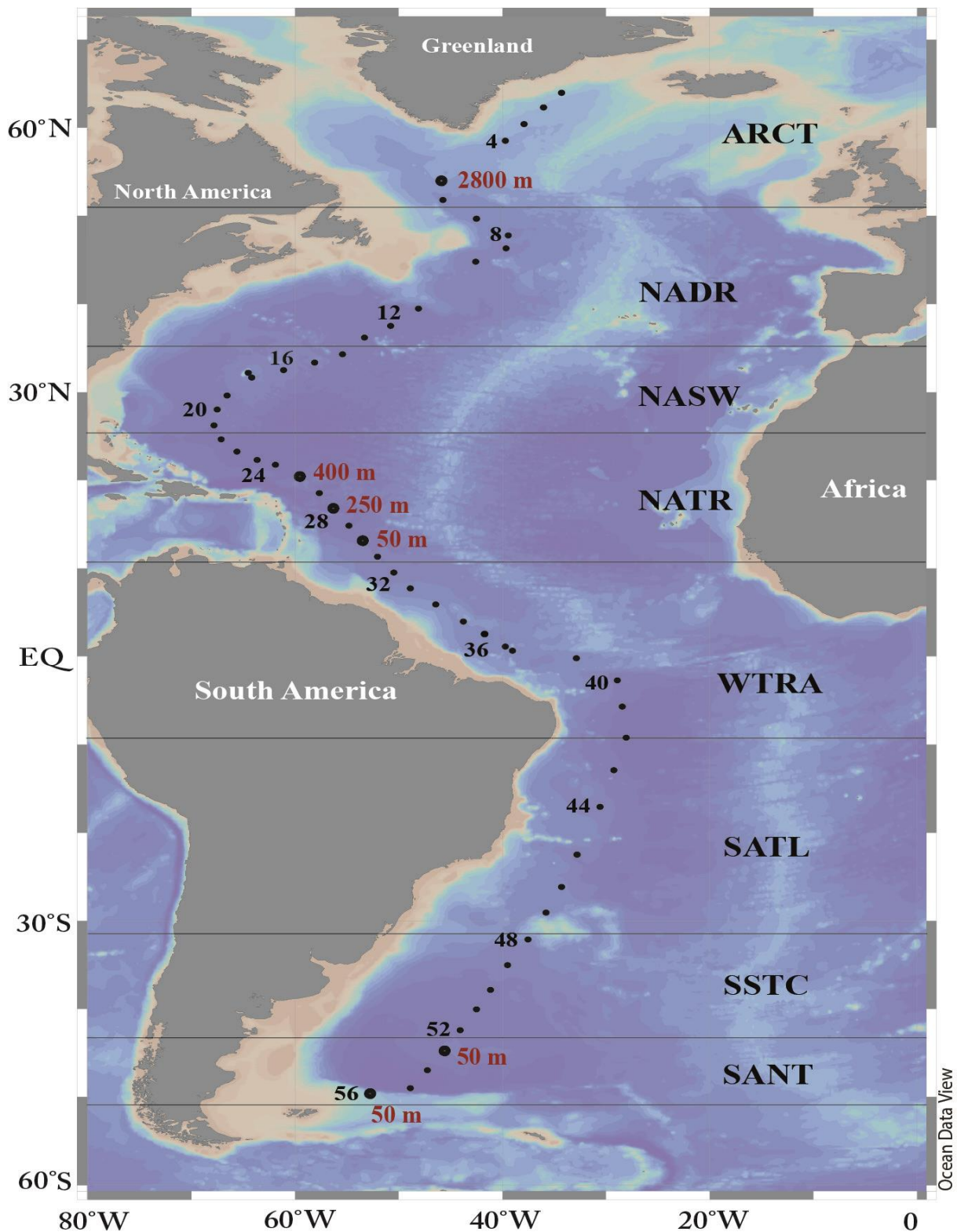
6. Tables and Figures

Figure 1. Transect of the Geotraces cruises 1-3 in April/July 2010 and February/March 2011 in the Atlantic Ocean. Horizontal black lines depict oceanic provinces following the Longhurst classification scheme (2006). Red labeled stations indicate samples and depths taken for establishing clone libraries.
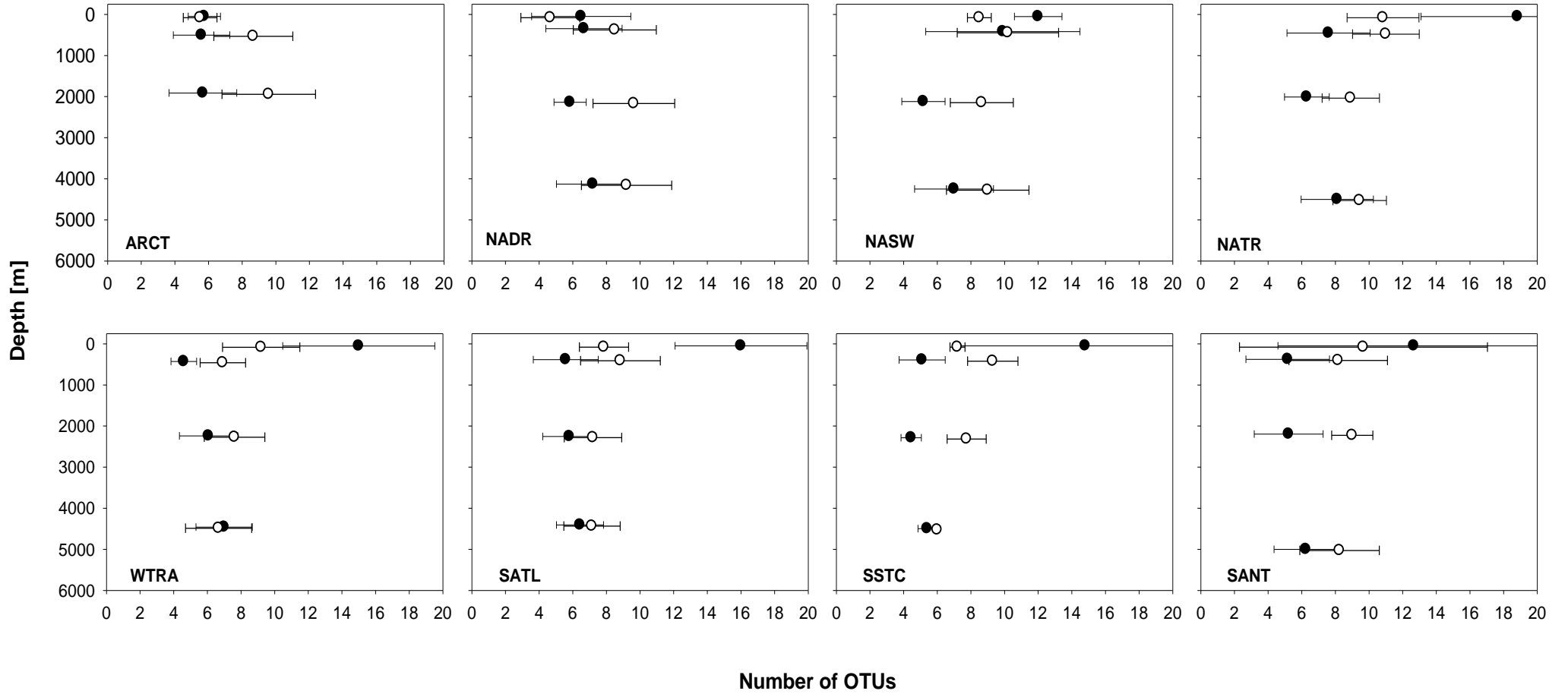
Figure 2. Mean number of OTUs obtained with the Archaea-specific primer pair 21F-FAM (black dots) and 958R-VIC (white dots) within each pelagic layer and province.
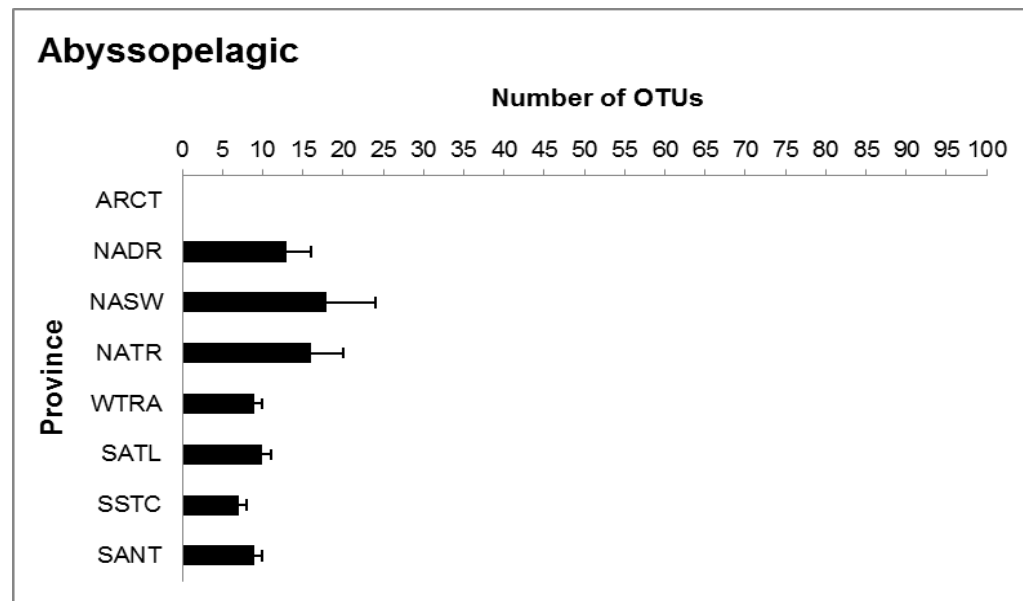
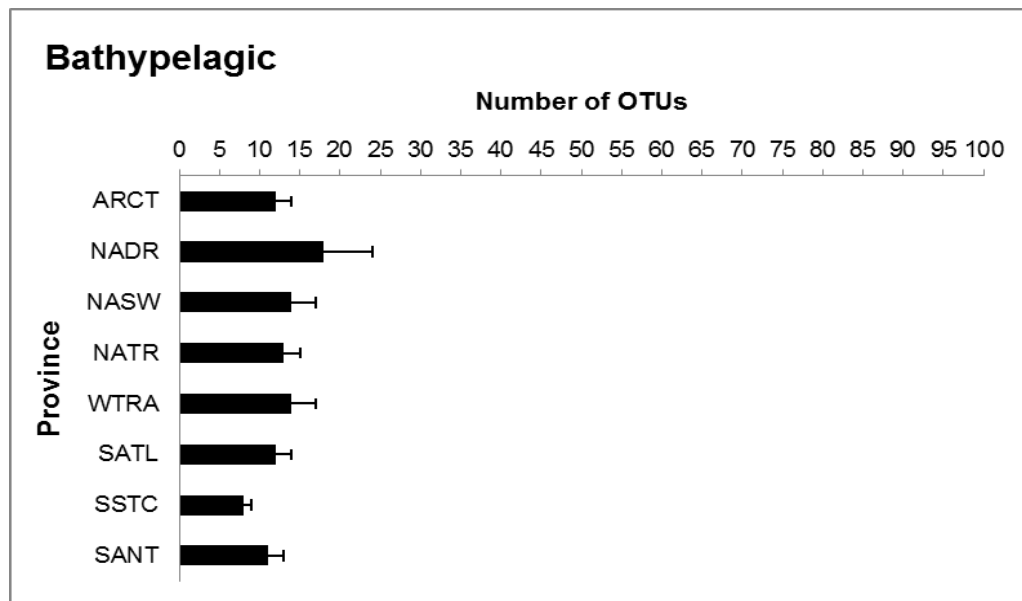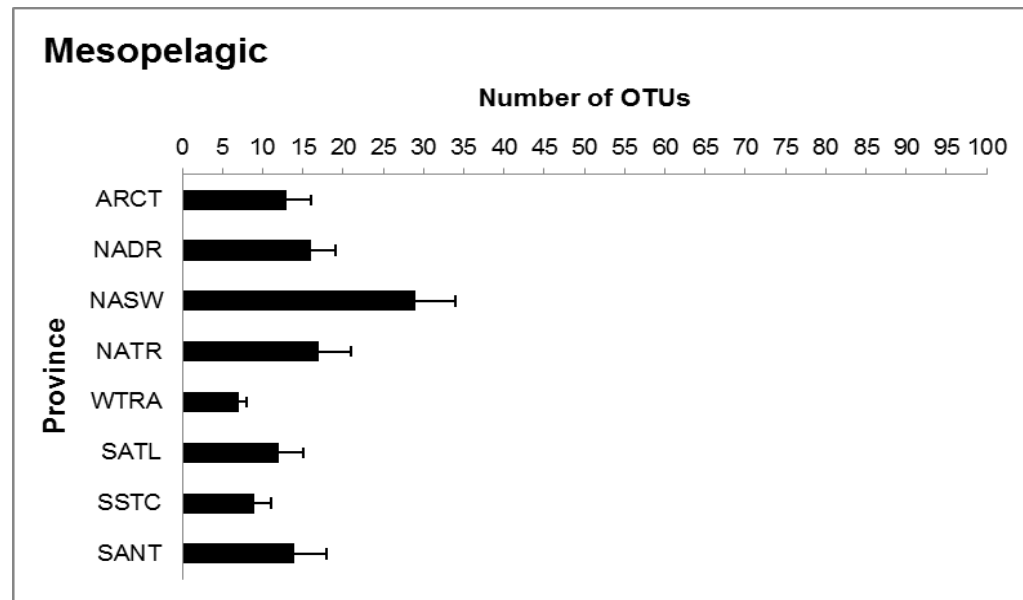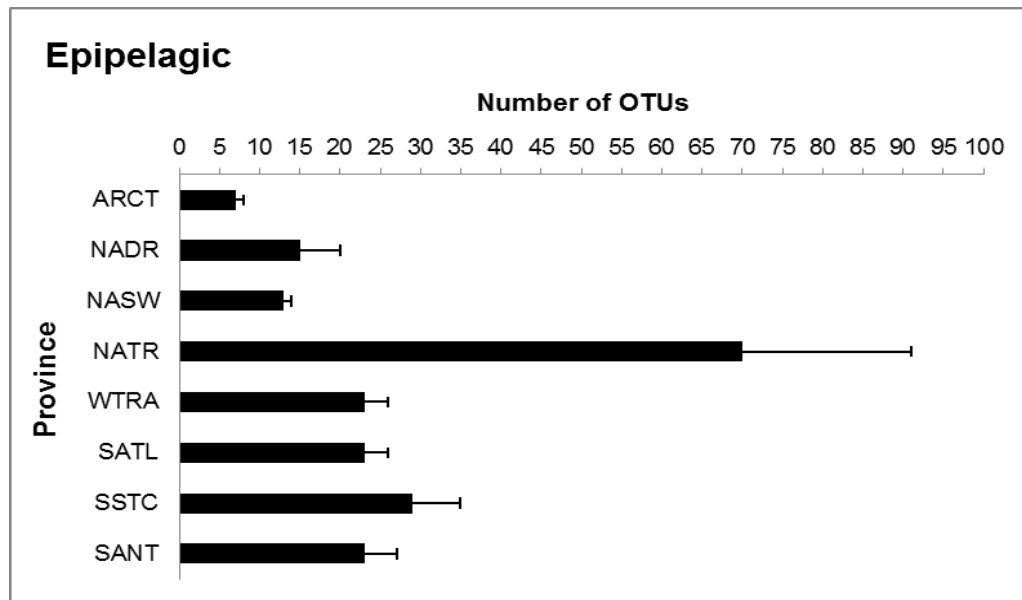**Figure 3A-D.** Estimated archaeal richness via Chao2 for each pelagic layer and province along the Geotraces 1-3 transect from 64.00°N to 49.55°S.
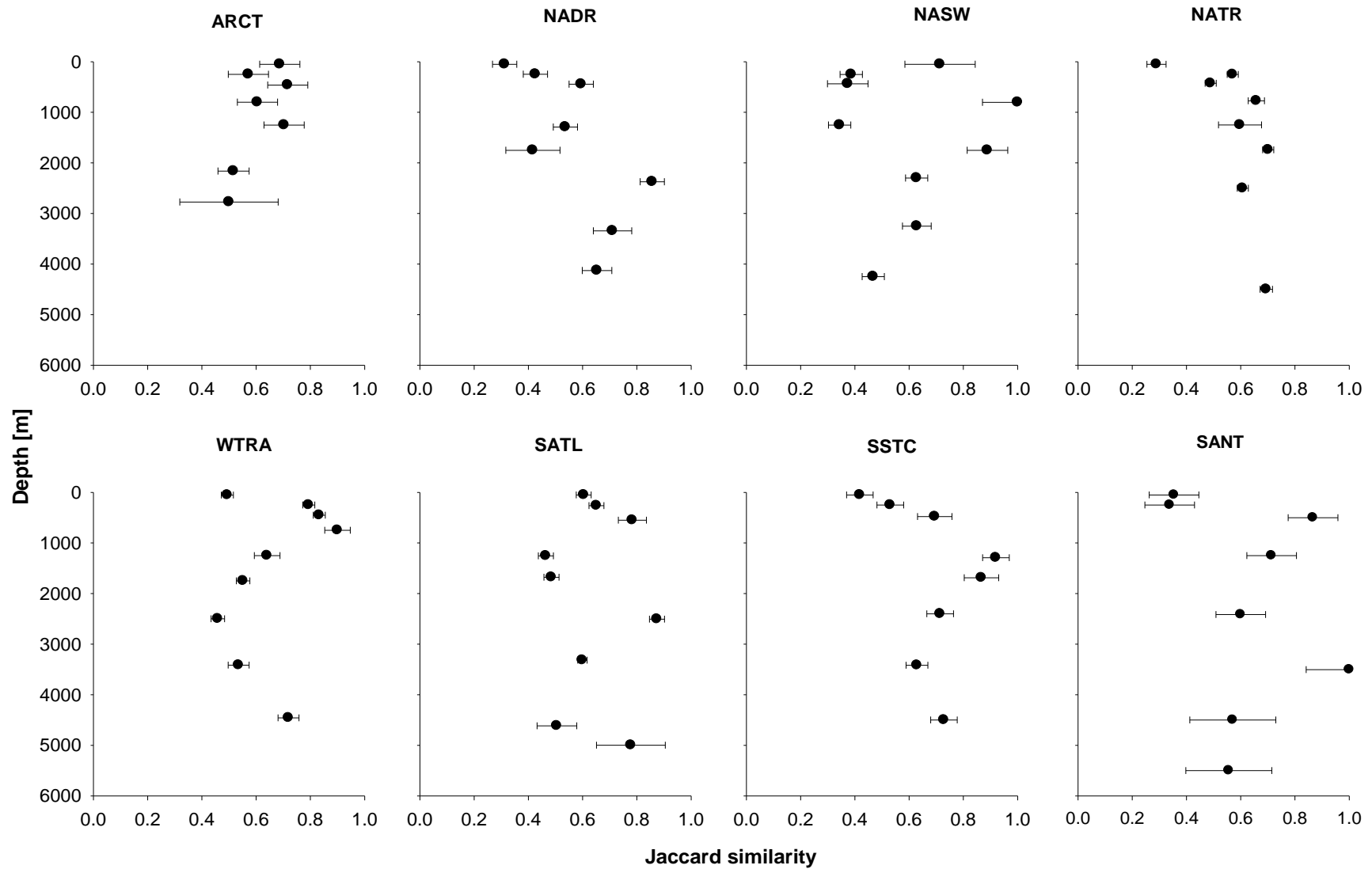
Figure 4. Variability of archaeal community composition within the individual depth layer, based on Jaccard similarity with standard error.
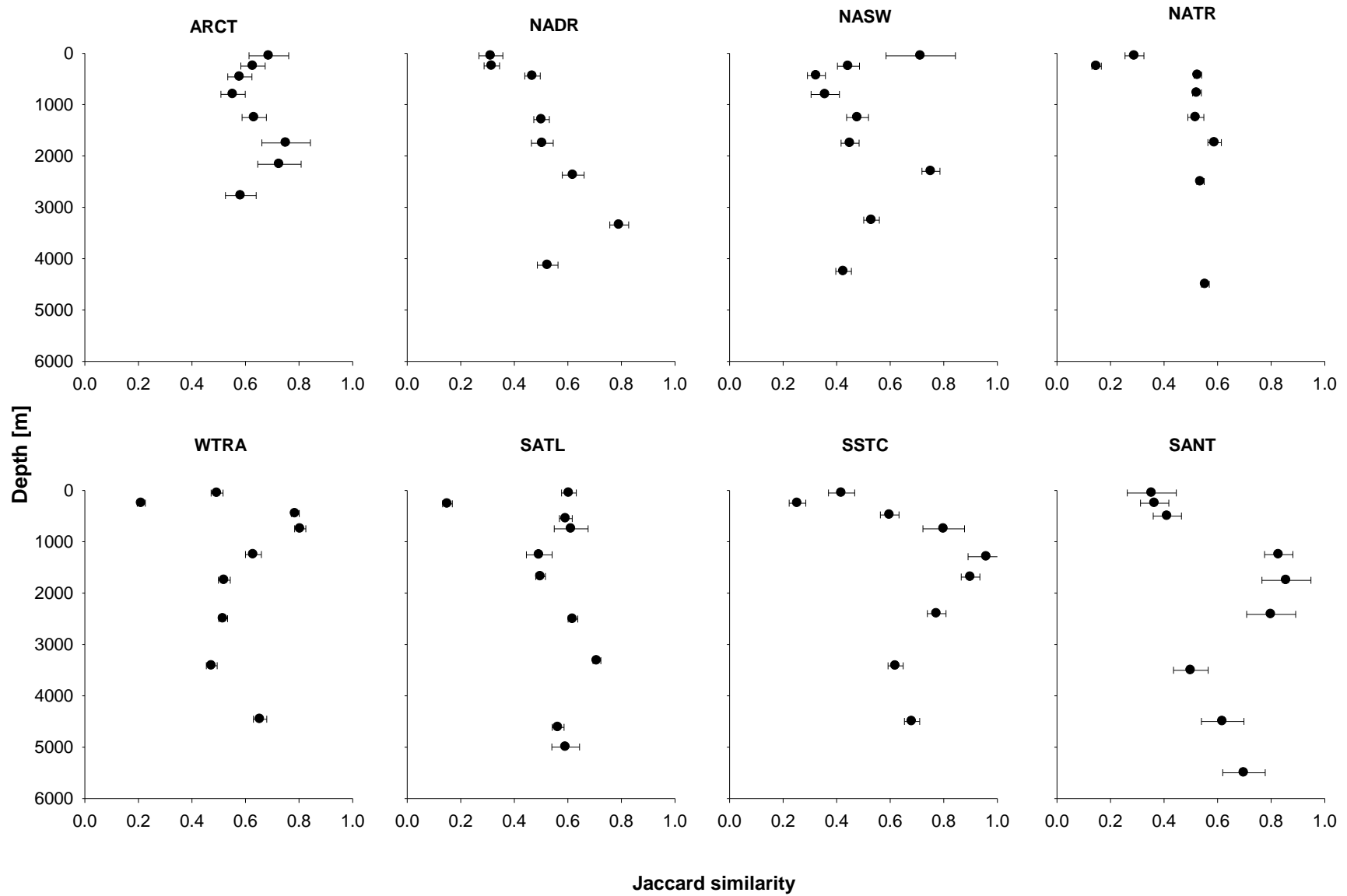
Figure 5. Changes in community composition from one depth layer to the one underneath, based on Jaccard similarity with standard error.

Figure 6. Changes in community composition throughout the water column in relation to the community composition of the 50 m layer for each oceanic province, based on Jaccard similarity with standard error.

Table S1. Primers used for the amplification of archaeal 16S rRNA and TOPO® TA® Cloning product.

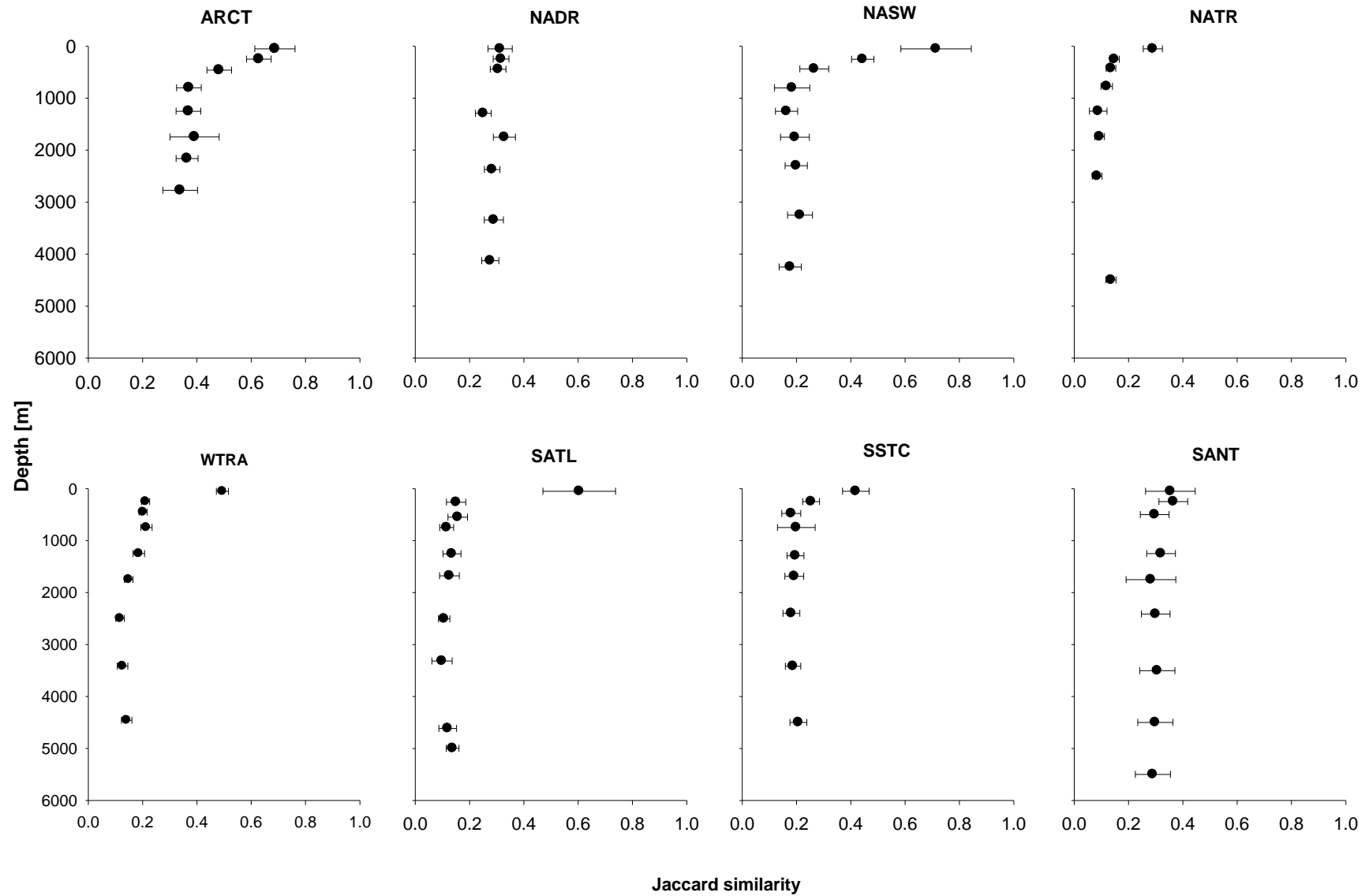| Target	Primer	Annealing temperature (°C)	Sequence 5' to 3'	Company	Reference
16S rRNA	21F-6FAM	55	TTCCGGTTGATCCYGCCGGA	ThermoScientific	DeLong, 1992
	958R-VIC	55	YCCGGCGTTGAMTCCAATT	ThermoScientific	DeLong 1992
pCR8®/GW/TOPO® vector	M13F	60	GTAAAACGACGGCCAG	Invitrogen	Invitrogen TOPO®TA®Kit
	M13R	60	CAGGAAACAGCTATGAC	Invitrogen	Invitrogen TOPO®TA®Kit

Table S2. Components and concentrations used for archaeal 16S rRNA PCR amplification and T-RFLP.

Component	Concentration	Company
PCR		
Taq Polymerase	5 U/µl	Fermentas
10x Taq Buffer Fermentas	500 mM KCl, 100 mM Tris HCl (pH 9.0 at 25°C), 15 mM MgCl2, and 1 % Triton X-100	Fermentas
$MgCl_2$	25 mM/1.25 ml	Fermentas
dNTP Mix	2 mM/ml	Fermentas
BSA	20 mg/ml	New England BioLabs
21F-6FAM	50 pmol	ThermoScientific
958R-VIC	50 pmol	ThermoScientific
T-RFLP		
HhaI	20 U/µl	New England BioLabs
Buffer	10x	New England BioLabs
BSA	100x	New England BioLabs

Table S3. P-values for Wilcoxon signed-ranks-test, calculated for pelagic layers within each province to detect significant differences in primer dependent OTU detection.

	Epipelagic 21F-FAM > 958R-VIC	Mesopelagic 21F-FAM < 958R-VIC	Bathypelagic 21F-FAM < 958R-VIC	Abyssopelagic 21F-FAM < 958R-VIC
ARCT	0.564	0.003	0.002	No abyssopelagic layer.
NADR	0.131	0.032	0.001	0.136
NASW	0.18	0.759	0.001	0.194
NATR	0.043	0.001	0.001	0.173
WTRA	0.008	0.001	0.003	1
SATL	0.018	0.002	0.001	0.257
SSTC	0.068	0.004	0.001	0.059
SANT	0.102	0.041	0.011	0.109
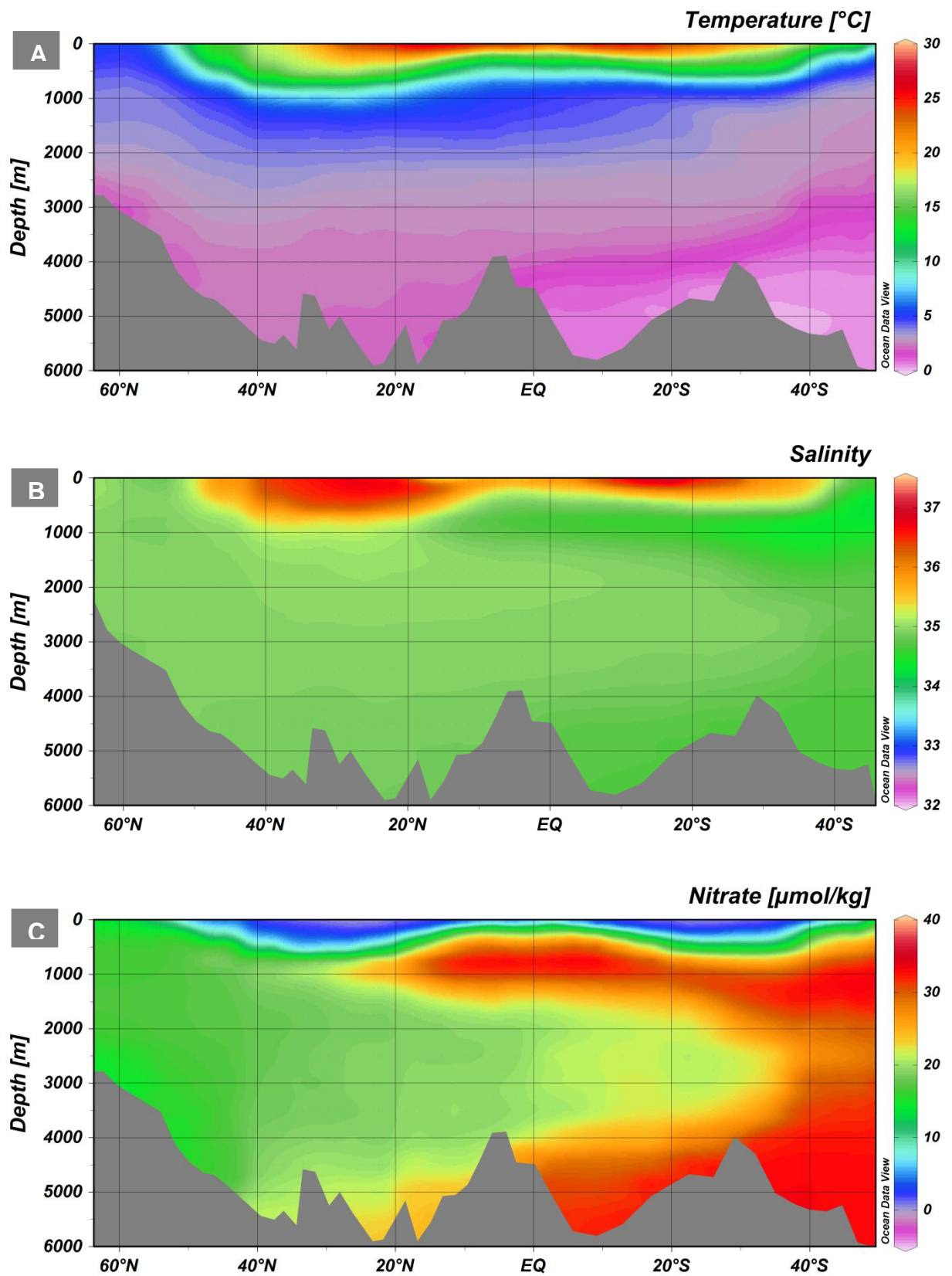
Figure S1. Physical and chemical characteristics of the Geotraces 1-3 transect for all depth layers. **A**. Mean Temperature [°C], **B**. Salinity, **C**. Nitrate [μmol kg^{-1}].
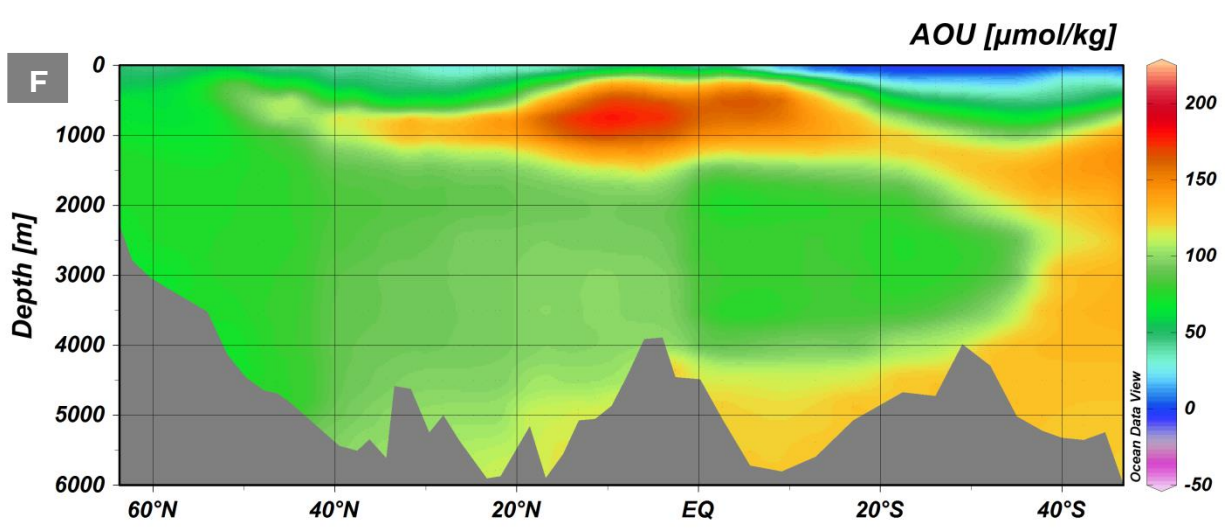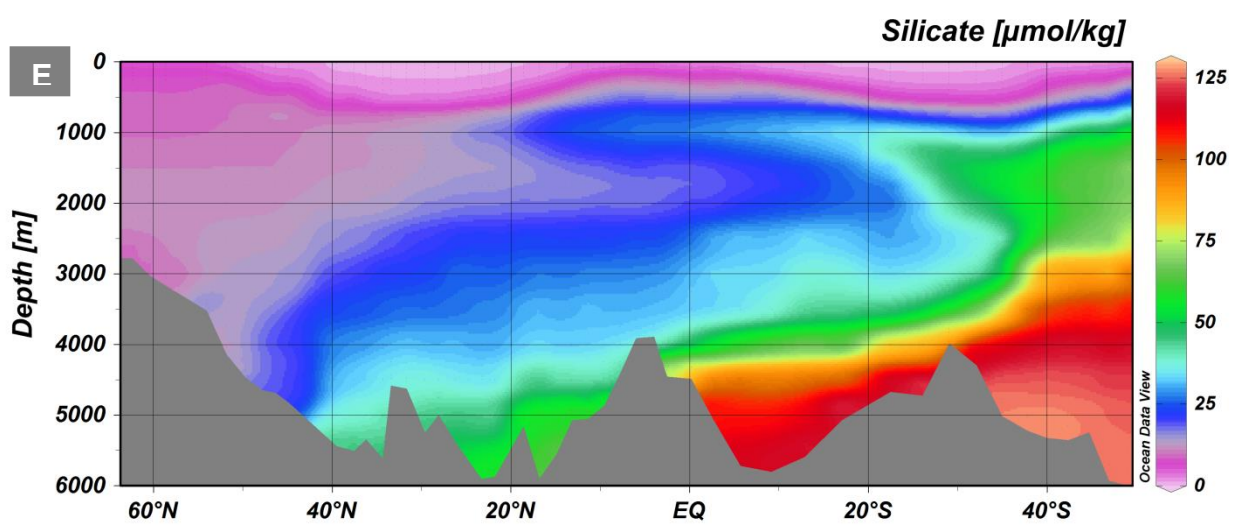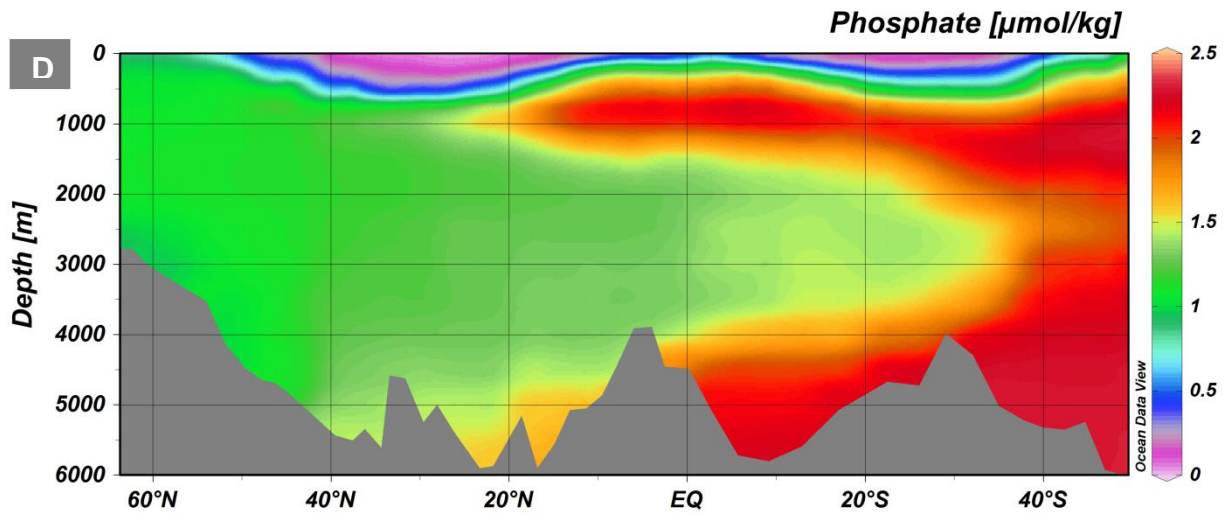
Figure S1. Physical and chemical characteristics of the Geotraces 1-3 transect for all depth layers. **D**. Phosphate [μmol kg⁻¹], **E**. Silicate [μmol kg⁻¹] and **F**. AOU [μmol kg⁻¹].
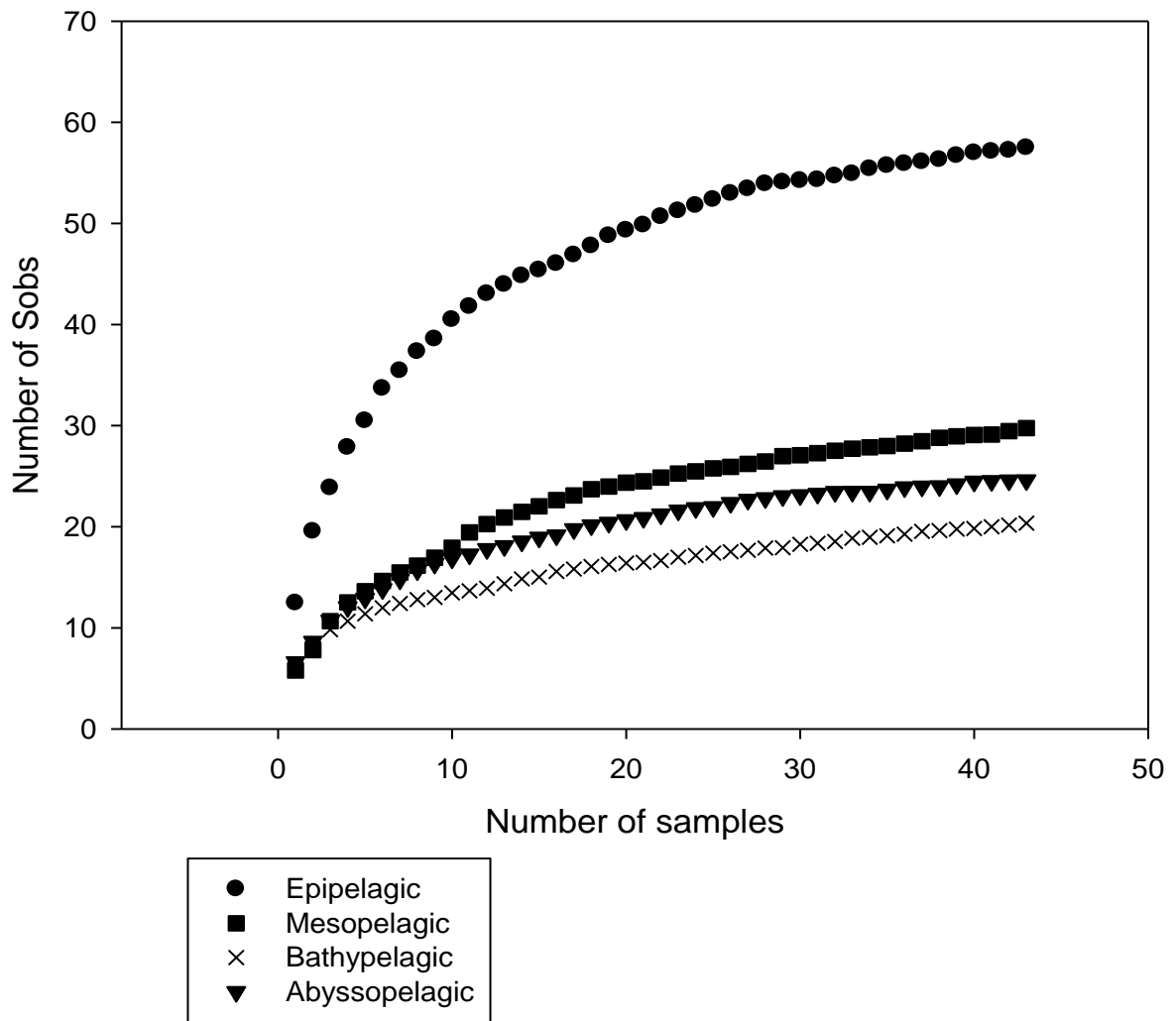
Figure S2. Computed rarefaction curves of species observed (Sobs) for each pelagic layer.
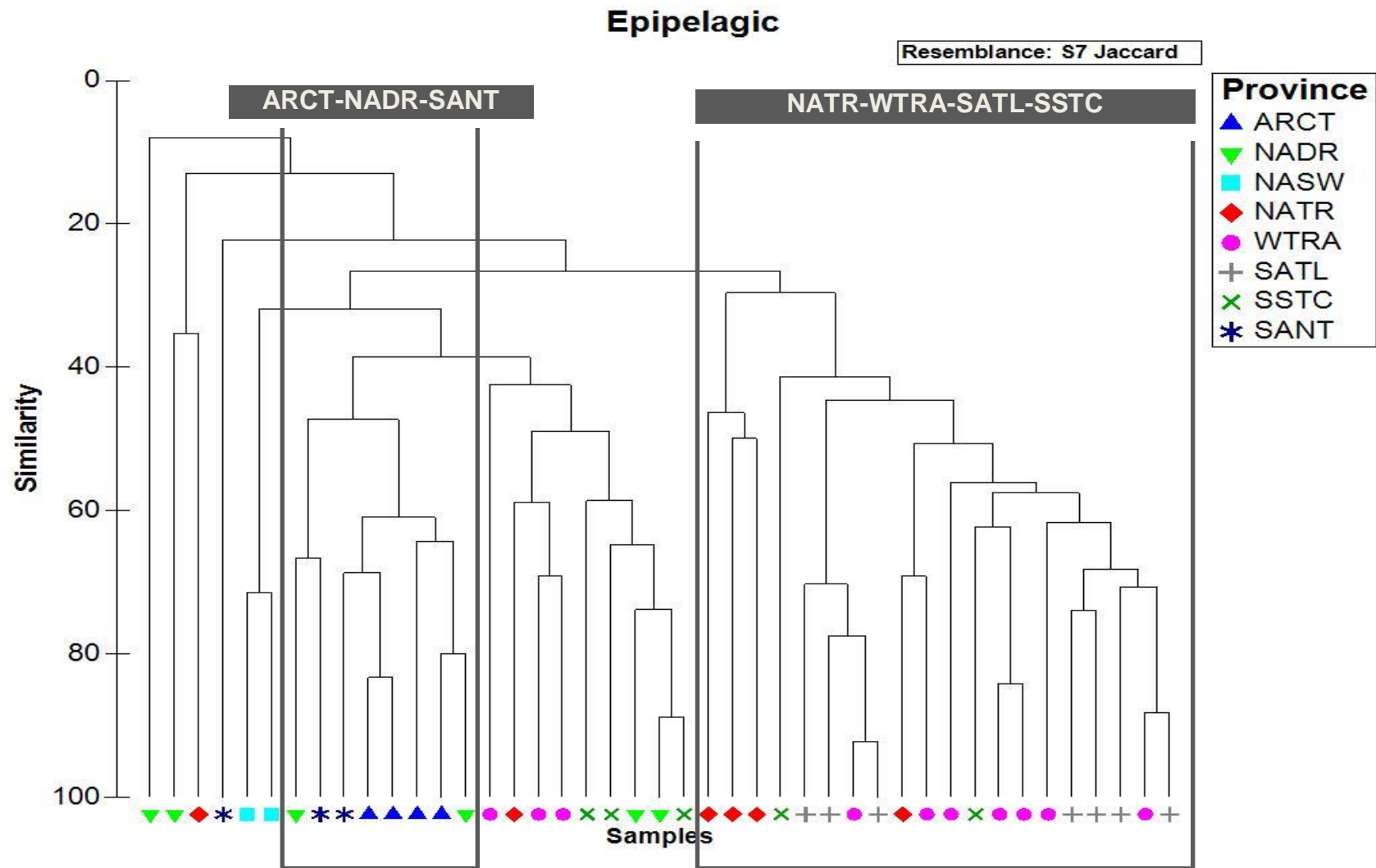
Figure S3A. Similarity tree of epipelagic samples, calculated with Jaccard similarity.
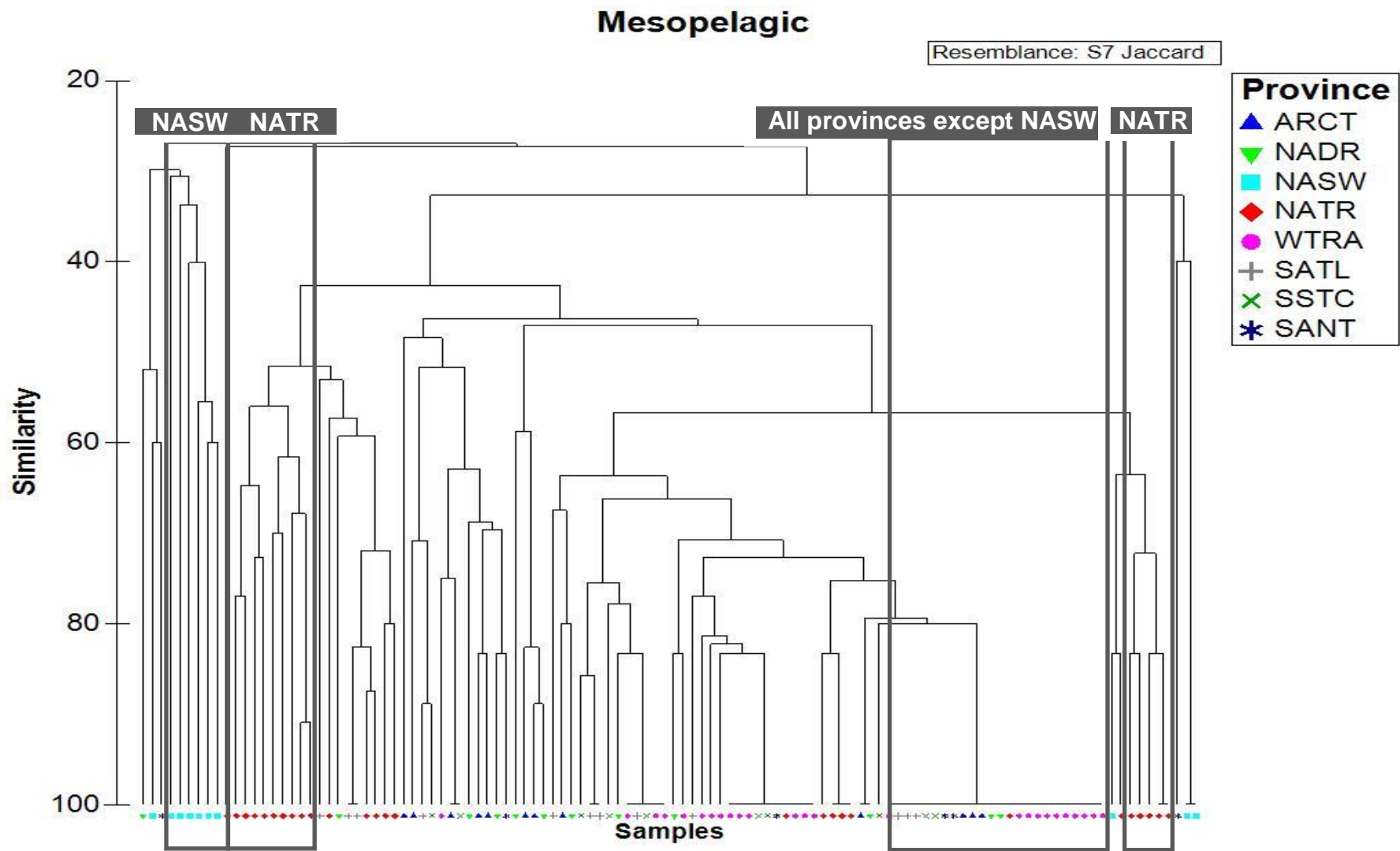
Figure S3B. Similarity tree of mesopelagic samples, calculated with Jaccard similarity.
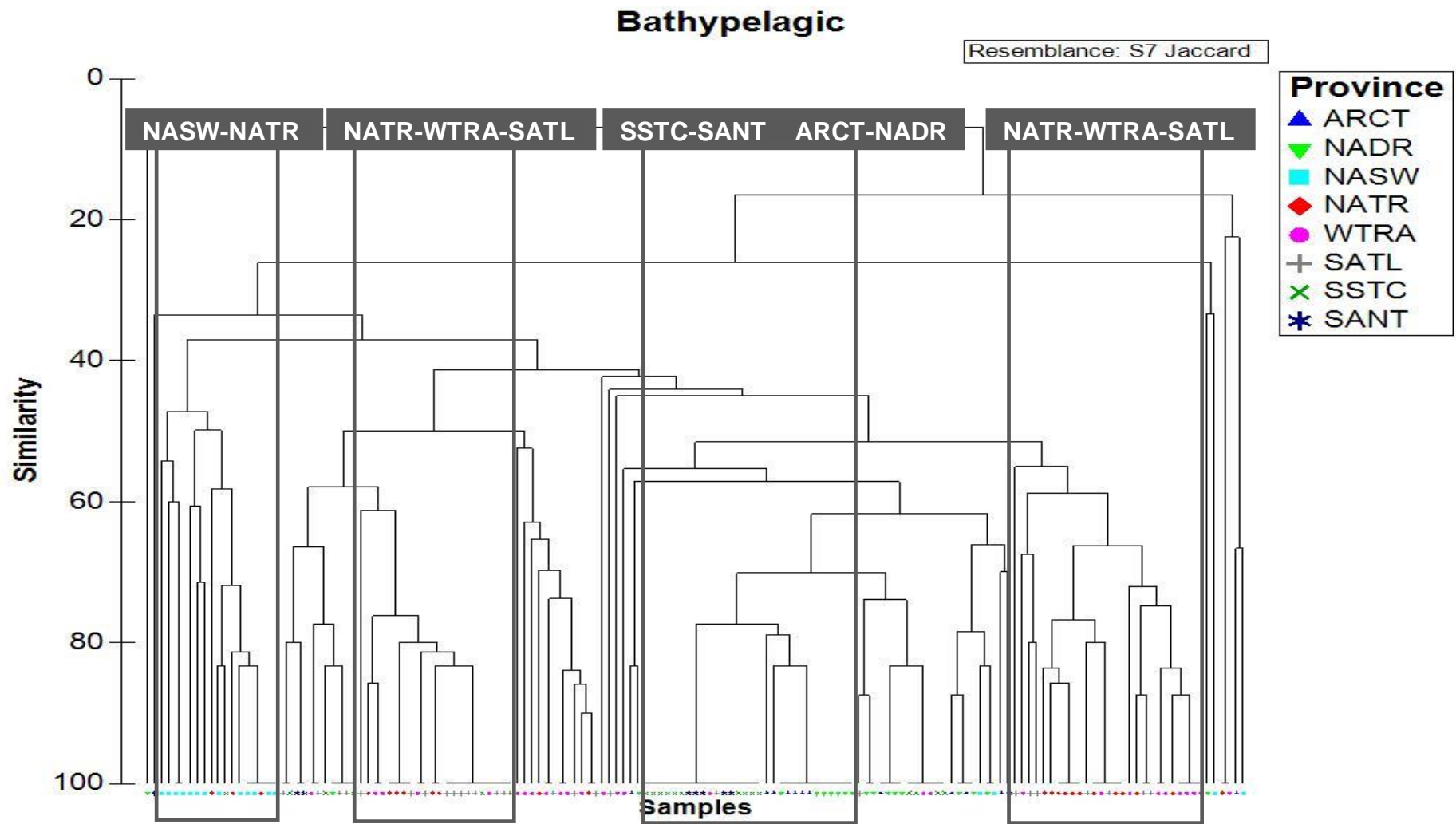
Figure S3C. Similarity tree of bathypelagic samples, calculated with Jaccard similarity.
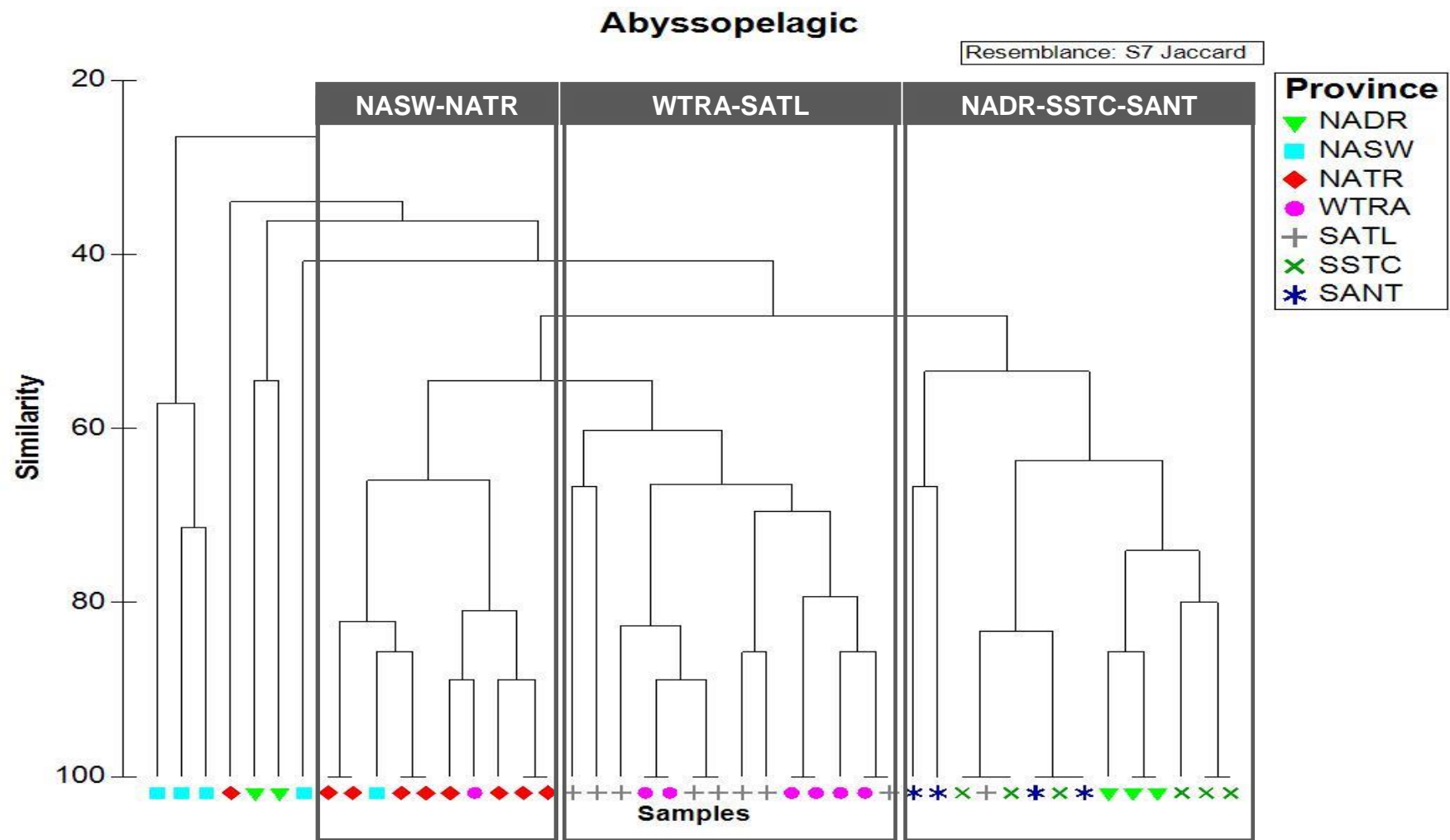
Figure S3D. Similarity tree of abyssopelagic samples, calculated with Jaccard similarity.
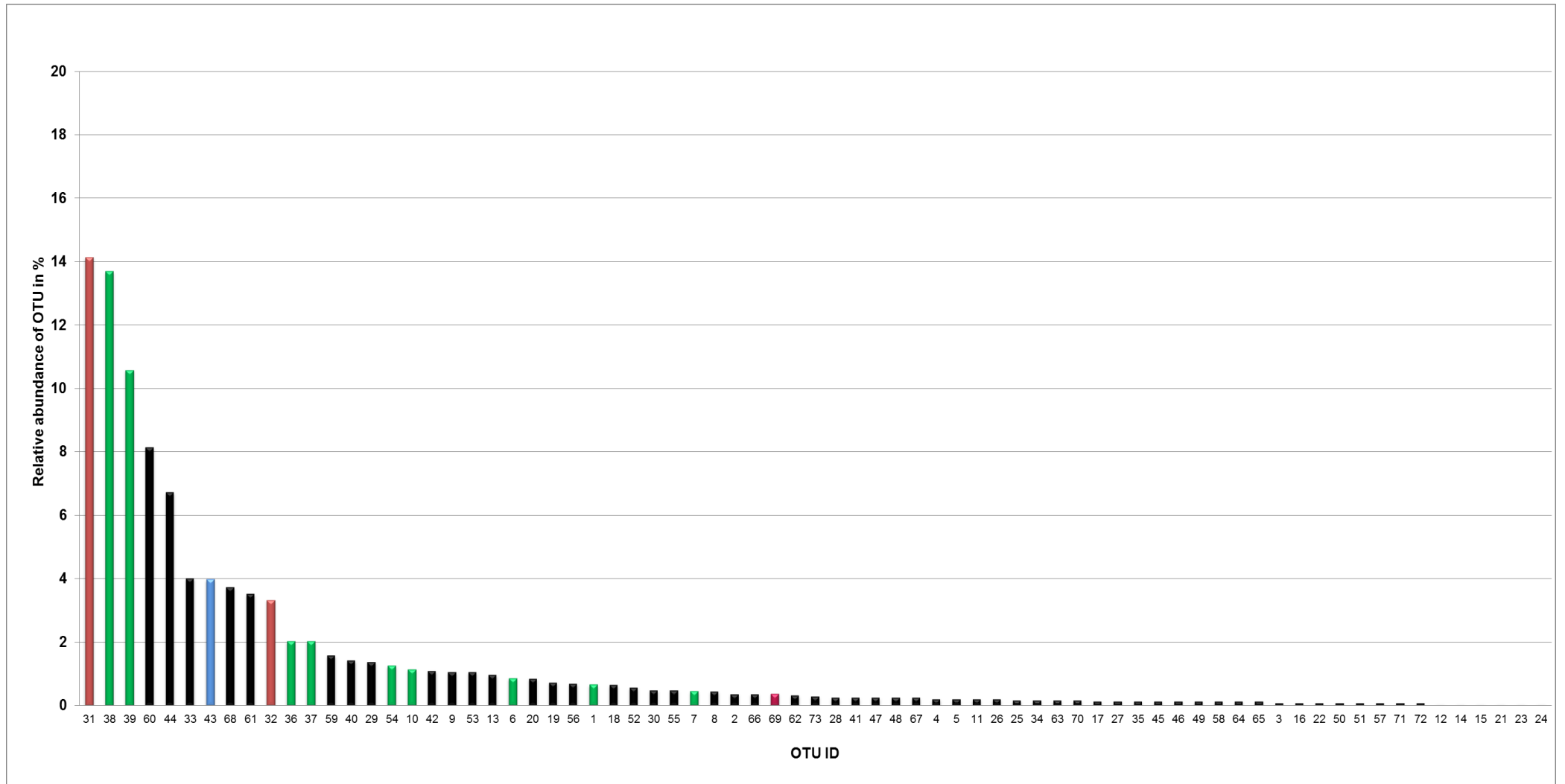
Figure S4. Relative abundance of 21F-FAM detected OTUs in total number of samples. Five OTUs constitute more than 50% of relative OTU abundance. Coloured bars indicate assigned sequences of established clone library: uncultured marine Archaea (red), Euryarchaeota (green) and Crenarchaeota (blue).

Appendix Table. Mean physical and chemical parameters for Geotraces cruise 1-3 transect, spanning from 64°00N to 49.00°S.

Depth range

| 50m	Temperature (°C) Mean	± SD	Salinity Mean	± SD	Phosphate (µmol kg-1) Mean	± SD	Silicate (µmol kg-1) Mean	± SD	Nitrite (µmol kg-1) Mean	± SD	Nitrate (µmol kg-1) Mean	± SD
ARCT	5.57	0.80	34.96	0.13	0.90	0.02	5.26	0.82	0.18	0.03	13.52	0.51
NADR	11.91	3.91	35.50	0.58	0.45	0.27	2.70	1.91	0.22	0.09	6.42	3.84
NASW	18.55	0.54	36.56	0.06	0.01	0.01	0.48	0.27	0.06	0.03	0.13	0.17
NATR	26.03	1.88	36.56	0.30	0.02	0.01	1.02	0.25	0.02	0.02	0.07	0.10
WTRA	27.21	2.31	36.14	0.24	0.09	0.18	1.17	0.60	0.08	0.13	1.16	2.57
SATL	24.48	3.37	36.65	0.62	0.04	0.03	0.51	0.16	0.03	0.07	0.00	0.00
SSTC	17.20	4.31	35.13	0.55	0.29	0.29	0.48	0.36	0.26	0.37	1.94	2.77
SANT	10.33	3.92	34.47	0.84	1.00	0.42	0.75	0.98	0.13	0.07	12.48	5.73

250m	Temperature (°C) Mean	± SD	Salinity Mean	± SD	Phosphate (µmol kg-1) Mean	± SD	Silicate (µmol kg-1) Mean	± SD	Nitrite (µmol kg-1) Mean	± SD	Nitrate (µmol kg-1) Mean	± SD
ARCT	5.12	0.98	34.98	0.10	1.04	0.04	7.80	0.65	0.05	0.02	15.98	0.61
NADR	9.81	4.22	35.33	0.49	0.90	0.38	7.20	3.88	0.04	0.01	14.16	5.45
NASW	17.32	0.68	36.45	0.11	0.21	0.06	1.50	0.27	0.02	0.01	4.12	0.86
NATR	18.44	0.53	36.59	0.07	0.23	0.15	1.55	0.53	0.02	0.01	4.96	2.53
WTRA	11.00	1.59	35.10	0.29	1.63	0.18	11.12	2.17	0.02	0.00	25.61	2.52
SATL	14.20	2.41	35.42	0.29	0.82	0.63	4.32	4.29	0.04	0.08	11.39	10.62
SSTC	9.79	4.71	34.83	0.70	1.12	0.62	5.49	3.54	0.02	0.01	16.10	9.83
SANT	5.00	3.24	34.23	0.30	1.65	0.38	12.68	6.82	0.02	0.01	24.01	5.63

375-600m	Temperature (°C) Mean	± SD	Salinity Mean	± SD	Phosphate (µmol kg-1) Mean	± SD	Silicate (µmol kg-1) Mean	± SD	Nitrite (µmol kg-1) Mean	± SD	Nitrate (µmol kg-1) Mean	± SD
ARCT	4.41	0.29	34.94	0.03	1.11	0.01	9.12	0.26	0.03	0.00	17.13	0.17
NADR	7.44	2.95	35.07	0.18	1.22	0.11	10.35	1.37	0.03	0.01	19.02	2.10
NASW	15.45	1.81	36.10	0.34	0.54	0.25	3.46	1.71	0.01	0.01	9.33	4.13
NATR	15.52	3.06	36.13	0.49	0.68	0.57	4.82	4.79	0.02	0.01	11.96	8.74
WTRA	8.31	1.25	34.79	0.17	2.05	0.17	17.44	3.04	0.02	0.01	32.34	2.66
SATL	9.89	1.34	34.82	0.13	1.31	0.35	8.13	4.47	0.05	0.08	19.32	5.81
SSTC	7.41	4.16	34.55	0.45	1.47	0.52	11.48	8.24	0.02	0.01	21.47	7.81
SANT	3.36	0.82	34.21	0.04	2.04	0.23	28.47	13.14	0.02	0.00	30.00	3.09

750-850m	Temperature (°C) Mean	± SD	Salinity Mean	± SD	Phosphate (µmol kg-1) Mean	± SD	Silicate (µmol kg-1) Mean	± SD	Nitrite (µmol kg-1) Mean	± SD	Nitrate (µmol kg-1) Mean	± SD
ARCT	3.84	0.24	34.89	0.03	1.10	0.01	9.06	0.11	0.02	0.01	16.80	0.11
NADR						no data available						
NASW	10.18	0.09	35.33	0.01	1.33	0.01	11.22	0.30	0.02	0.02	21.48	0.02
NATR	8.64	1.48	35.12	0.22	1.74	0.31	16.68	4.67	0.02	0.01	27.44	4.22
WTRA	5.57	0.53	34.59	0.06	2.33	0.04	27.25	2.14	0.01	0.01	35.51	0.59
SATL	5.22		34.38		2.03		23.29		0.00		30.20	
SSTC	3.69		34.23		2.04		25.93		0.00		30.17	
SANT						no data available						

1250m	Temperature (°C) Mean	± SD	Salinity Mean	± SD	Phosphate (µmol kg-1) Mean	± SD	Silicate (µmol kg-1) Mean	± SD	Nitrite (µmol kg-1) Mean	± SD	Nitrate (µmol kg-1) Mean	± SD
ARCT	3.74	0.15	34.92	0.03	1.12	0.01	10.35	0.22	0.02	0.01	17.12	0.09
NADR	4.03	0.38	34.93	0.03	1.14	0.02	10.67	0.40	0.02	0.00	17.59	0.28
NASW	4.99	0.23	35.04	0.03	1.22	0.01	12.00	0.24	0.01	0.01	18.88	0.20
NATR	5.29	0.18	35.06	0.03	1.36	0.05	14.81	1.39	0.02	0.01	20.96	0.68
WTRA	4.66	0.28	34.88	0.05	1.77	0.07	22.94	1.63	0.01	0.01	26.67	0.78
SATL	3.59	0.49	34.63	0.14	2.05	0.15	40.17	10.90	0.02	0.03	30.48	2.09
SSTC	2.92	0.22	34.48	0.11	2.26	0.03	55.73	10.01	0.01	0.01	33.19	0.43
SANT	2.58	0.27	34.57	0.09	2.32	0.04	69.48	11.48	0.02	0.00	33.81	0.72

1750m	Temperature (°C) Mean	± SD	Salinity Mean	± SD	Phosphate (µmol kg-1) Mean	± SD	Silicate (µmol kg-1) Mean	± SD	Nitrite (µmol kg-1) Mean	± SD	Nitrate (µmol kg-1) Mean	± SD
ARCT	3.41		34.93		1.11		11.55		0.03		16.98	
NADR	3.57	0.28	34.92	0.02	1.15	0.02	11.79	0.40	0.02	0.00	17.62	0.38
NASW	3.97	0.12	34.98	0.02	1.19	0.01	13.05	0.57	0.01	0.00	18.26	0.08
NATR	3.99	0.09	35.00	0.01	1.24	0.03	14.77	0.73	0.02	0.02	18.96	0.29
WTRA	3.99	0.17	34.98	0.01	1.30	0.03	16.26	1.04	0.01	0.01	19.77	0.49
SATL	3.43	0.37	34.84	0.16	1.63	0.35	32.50	15.61	0.02	0.04	24.32	4.96
SSTC	2.79	0.13	34.66	0.09	2.13	0.10	62.22	5.02	0.02	0.01	31.24	1.38
SANT	1.98		34.70		2.26		91.93		0.02		32.89	

2000-2700m	Temperature (°C)		Salinity		Phosphate (µmol kg-1)		Silicate (µmol kg-1)		Nitrite (µmol kg-1)		Nitrate (µmol kg-1)	
	Mean	± SD	Mean	± SD	Mean	± SD	Mean	± SD	Mean	± SD	Mean	± SD
ARCT	2.91	0.58	34.91	0.02	1.06	0.10	10.57	2.29	0.03	0.01	15.97	1.71
NADR	3.22	0.26	34.92	0.01	1.13	0.02	12.68	0.93	0.02	0.00	17.21	0.28
NASW	3.48	0.27	34.95	0.01	1.21	0.04	16.86	3.50	0.02	0.01	18.51	0.45
NATR	3.08	0.05	34.96	0.01	1.29	0.03	22.89	1.34	0.02	0.01	19.43	0.31
WTRA	3.00	0.09	34.94	0.01	1.32	0.07	25.58	4.63	0.01	0.01	19.90	0.91
SATL	2.95	0.08	34.92	0.01	1.41	0.04	31.40	2.74	0.03	0.06	21.15	0.60
SSTC	2.71	0.40	34.84	0.04	1.73	0.17	53.31	14.46	0.02	0.01	25.67	2.36
SANT	1.96	0.59	34.77	0.05	2.02	0.17	83.03	21.68	0.01	0.01	29.57	2.35

2700-3500m	Temperature (°C)		Salinity		Phosphate (µmol kg-1)		Silicate (µmol kg-1)		Nitrite (µmol kg-1)		Nitrate (µmol kg-1)	
	Mean	± SD	Mean	± SD	Mean	± SD	Mean	± SD	Mean	± SD	Mean	± SD
ARCT	2.38	0.28	34.90	0.02	1.02	0.05	10.77	2.04	0.02	0.00	15.34	0.87
NADR	2.58	0.30	34.91	0.01	1.12	0.01	15.64	1.32	0.02	0.00	16.75	0.44
NASW	2.66	0.30	34.92	0.02	1.24	0.02	23.65	3.34	0.02	0.01	18.58	0.16
NATR							no data available					
WTRA	2.50	0.11	34.91	0.00	1.33	0.01	31.24	0.75	0.02	0.01	19.87	0.32
SATL	2.60	0.15	34.90	0.01	1.41	0.04	36.45	4.01	0.03	0.05	21.19	0.59
SSTC	1.34	0.36	34.74	0.03	2.08	0.14	98.40	13.58	0.01	0.01	30.52	1.74
SANT	1.16	0.29	34.72	0.02	2.17	0.07	106.51	7.17	0.00	0.00	31.58	0.66

3500-5000m	Temperature (°C)		Salinity		Phosphate (µmol kg-1)		Silicate (µmol kg-1)		Nitrite (µmol kg-1)		Nitrate (µmol kg-1)	
	Mean	± SD	Mean	± SD	Mean	± SD	Mean	± SD	Mean	± SD	Mean	± SD
ARCT							no sample available					
NADR	2.20	0.13	34.90	0.00	1.11	0.07	17.58	4.80	0.02	0.01	16.54	1.05
NASW	2.26	0.06	34.89	0.01	1.32	0.04	33.06	3.11	0.02	0.01	19.63	0.53
NATR	2.23	0.06	34.89	0.01	1.39	0.06	37.86	5.06	0.01	0.01	20.56	0.89
WTRA	1.89	0.64	34.85	0.07	1.57	0.32	55.63	30.51	0.01	0.01	23.15	4.46
SATL	1.58	0.74	34.80	0.08	1.78	0.29	75.14	30.18	0.01	0.02	26.36	4.12
SSTC	0.46	0.34	34.68	0.02	2.24	0.04	121.18	6.85	0.01	0.01	32.61	0.43
SANT	0.44	0.09	34.68	0.00	2.27	0.05	121.71	1.30	0.00	0.00	32.72	0.08

>5000m	Temperature (°C) Mean	± SD	Salinity Mean	± SD	Phosphate (µmol kg-1) Mean	± SD	Silicate (µmol kg-1) Mean	± SD	Nitrite (µmol kg-1) Mean	± SD	Nitrate (µmol kg-1) Mean	± SD
ARCT							no data available					
NADR							no data available					
NASW							no data available					
NATR							no data available					
WTRA							no data available					
SATL	0.78	0.03	34.71	0.00	2.11	0.01	109.24	1.72	0.01	0.00	30.90	0.20
SSTC	0.30		34.67		2.28		124.79		0.03		33.02	
SANT	0.34	0.01	34.67	0.00	2.29	0.03	125.52	0.46	0.01	0.00	32.96	0.04

7. Acknowledgements

I kindly want to thank Gerhard J. Herndl for giving me the opportunity to write my diploma thesis at the Department of Marine Biology at the University of Vienna. Thanks to Kristin Bergauer for her supervision and to Christian Baranyi for his expertise in lab works and statistics. Thanks to the people at the department, for having a great time during lab works and lunch breaks; to my "Arbeitsehefrau" Katharina, to my family and friends. To Walter: for his encouragement and patience. And last but not least: to Jojo and Tobi. AEWB.GL!

8. References

Agogue H, Lamy D, Neal P, Sogin M, Herndl G (2011) Water mass-specificity of bacterial communities in the North Atlantic revealed by massively parallel sequencing. Mol Ecol 20:258-274

Aller J, Kemp P (2008) Are Archaea ineherently less diverse than Bacteria in the same environments? Fems Microbiol Ecol 65:74-87

Amano-Sato C, Akiyama S, Uchida M, Shimada K, Utsumi M (2013) Archaeal distribution and abundance in water masses of the Arctic Ocean, Pacific sector. Aquat Microb Ecol 69:101-112

Bano N, Ruffin S, Ransom B, Hollibaugh J (2004) Phylogenetic composition of Arctic Ocean archaeal assemblages and comparison with Antarctic assemblages. Appl Environ Microb 70:781-789

Brochier-Armanet C, Boussau B, Gribaldo S, Forterre P (2008) Mesophilic Crenarchaeota: proposal for a third archaeal phylum, the Thaumarchaeota. Nat Rev Microbiol 6:245-252

Church M, DeLong E, Ducklow H, Karner M, Preston C, Karl D (2003) Abundance and distribution of planktonic Archaea and Bacteria in the waters west of the Antarctic Peninsula. Limnol Oceanogr 48:1893-1902

Cole J, Chai B, Marsh T, Farris R, Wang Q, Kulam S, Chandra S, McGarrell D, Schmidt T, Garrity G, Tiedje J (2003) The Ribosomal Database Project (RDP-II): previewing a new autoaligner that allows regular updates and the new prokaryotic taxonomy. Nucleic Acids Res 31:442-443

De Corte D, Yokokawa T, Varela MM, Agogue H, Herndl GJ (2009) Spatial distribution of Bacteria and Archaea and amoA gene copy numbers throughout the water column of the Eastern Mediterranean Sea. The ISME journal 3:147-158

DeLong E (1992) Archaea in coastal marine environments. P Natl Acad Sci USA 89:5685-5689

DeLong E, Preston C, Mincer T, Rich V, Hallam S, Frigaard N, Martinez A, Sullivan M, Edwards R, Brito B, Chisholm S, Karl D (2006) Community genomics among stratified microbial assemblages in the ocean's interior. Science 311:496-503

Fuhrman J, McCallum K, Davis A (1992) Novel major archaebacterial group from marine plankton. Nature 356:148-149

Fuhrman J, Steele J, Hewson I, Schwalbach M, Brown M, Green J, Brown J (2008) A latitudinal diversity gradient in planktonic marine bacteria. PNAS 105:7774-7778

Ghiglione J, Galand P, Pommier T, Pedrós-Alio C, Maas E, Bakker K, Bertilson S, Kirchman D, Lovejoy C, Yager P, Murray A (2012) Pole-to-pole biogeography of surface and deep marine bacterial communities. PNAS 43:17633-17638

Gotelli NCR (2001) Quantifying biodiversity: procedures and pitfalls in the measurement and comparison of species richness. Ecology letters 4:379-391

Helder W, De Vries R (1979) An automatic phenol-hypochlorite method for the detection of ammonia in sea- and brackish waters. Netherlands Journal of Sea Research 13:154-160

Hewson I, Steele J, Capone D, Fuhrman J (2006) Remarkable heterogeneity in meso- and bathypelagic bacterioplankton asseblage composition. Limnol Oceanogr 51:1274-1281

Hillebrand H (2004) Strength, slope and variability of marine latitudinal gradients. Mar Ecol Prog Ser 273:251-267

Karner M, DeLong E, Karl D (2001) Archaeal dominance in the mesopelagic zone of the Pacific Ocean. Nature 409:507-510

Lekunberri I, Sintes E, DeCorte D, Yokokawa T, Herndl G (2013) Spatial patterns of bacterial and archaeal communities along the Romanche Fracture Zone (tropical Atlantic). Fems Microbiol Ecol

Longhurst AR (2006) Ecological Geography of the Sea. Academic Press: San Diego, CA,USA

Massana R, DeLong E, Pedros-Alio C (2000) A few cosmopolitan phylotypes dominate planktonic archaeal assemblages in widely different oceanic provinces. Appl Environ Microb 66:1777-1787

Massana R, Murray A, Preston C, DeLong E (1997) Vertical distribution and phylogenetic characterization of marine planktonic Archaea in the Santa Barbara Channel. Appl Environ Microb 63:50-56

Massana R, Taylor L, Murray A, Wu K, Jeffrey W, DeLong E (1998) Spatial distribution and temporal variation of planktonic archaea in the Gerlache Strait, Antarctica, during early spring. Limnol Oceanogr 43:607-617

Moeseneder M, Winter C, Arrieta J, Herndl G (2001) Terminal-restriction fragment length polymorphism (T-RFLP) screening of a marine archaeal clone library to determine the different phylotypes. J Microbiol Meth 44:159-172

Murphy J, Riley J (1962) A modified single solution method for the determination of phosphate in natural waters. Analytica Chimica Acta 27:31-36

Parsons T, Maita Y, Lalli Y (1984) A manual of chemical and biological methods for seawater analysis. Pergamon press

Roy K, Jablonski D, Valentine J, Rosenberg G (1998) Marine latitudinal diversity gradients: tests of causal hypotheses. P Natl Acad Sci USA 95:3699-3702

Schattenhofer M, Fuchs B, Amann R, Zubkov M, Tarran G, Pernthaler J (2009) Latitudinal distribution of prokaryotic picoplankton populations in the Atlantic Ocean. Environ Microbiol 11:2078-2093

Sintes E, Witte H, Stodderegger K, Steiner P, Herndl G (2013) Temporal dynamics in the free-living bacterial community composition in the coastal North Sea. Fems Microbiol Ecol 83:413-424

Teira E, Van Aken H, Veth C, Herndl G (2006) Archaeal uptake of enantiomeric amino acids in the meso- and bathypelagic waters of the North Atlantic. Limnol Oceanogr 51:60-69

Tomczak M, Godfrey S (2003) Regional Oceanography: An Introduction.229-298

Van Aken H (2010) Hydrography Geotraces, NW‑Atlantic, 2010, cruises PE319 & PE321, a first hydrographic description.

Van Aken H (2011) Geotraces, the hydrography of the Western Atlantic Ocean, cruises 64PE319, 64PE321, and 74JC057.

Varela M, Van Aken H, Sintes E, Herndl G (2008) Latitudinal trends of Crenarchaeota and Bacteria in the meso- and bathypelagic water masses of the Eastern North Atlantic. Environ Microbiol 10:110-124

Wuchter C, Abbas B, Coolen M, Herfort L, Van Bleijswijk J, Timmers P, Strous M, Teira E, Herndl G, Middelburg J, Schouten S, Sinninghe Damste J (2006) Archaeal nitrification in the ocean. P Natl Acad Sci USA 103:12317-12322

Curriculum Vitae

Claudia Christine Sulzer

Education

2013	Diploma thesis at the Department of Marine Biology, University of Vienna: "Archaeal community profiling using T-RFLP along a latitudinal transect in the Atlantic Ocean"
2005-2013	Study of Biology/Ecology at the University of Vienna; specialization in Marine Biology
2004-2005	Study of Translation and Interpretation at the University of Vienna; languages: German, English and Spanish
1999-2004	Höhere Lehranstalt für wirtschaftliche Berufe Biedermannsdorf , Lower Austria
1995-1999	Bundesrealgymnasium Perchtoldsdorf, Lower Austria
1991-1995	Elementary school Brunn am Gebirge, Lower Austria

Internships

2012	Research cruise (MEDEA-2) in the Atlantic Ocean with RV Pelagia; measurement of ectoenzymatic activity
2011	"Effect of Black Carbon on bacterial communities", students' course at the NIOZ, Texel, The Netherlands
2011	Internship at the Department of Marine Biology, University of Vienna
2010	"Marine flora and fauna of the Mediterranean Sea", students' course at the Department of Marine Biology, Rovinj, Croatia
2010	"Impact of viral activity on bacterial growth rates", students' course at the Department of Marine Biology, Piran, Slovenia
2010	Biology and systematics of neotropical amphibians, tropical rainforest French Guiana
2009	"Central European biocenoses", Riegersburg, Lower Austria